

MICROGRID WITH ELECTRIC VEHICLES

BY

BEHROUZ AZIMIAN

A THESIS  
SUBMITTED TO THE FACULTY OF  
ALFRED UNIVERSITY

IN PARTIAL FULFILLMENT OF THE REQUIREMENTS  
FOR THE DEGREE OF

MASTER OF SCIENCE

IN

ELECTRICAL ENGINEERING

ALFRED, NEW YORK

MAY, 2019

Alfred University theses are copyright protected and may be used for education or personal research only. Reproduction or distribution in part or whole is prohibited without written permission from the author.

Signature page may be viewed at Scholes Library,  
New York State College of Ceramics, Alfred University,  
Alfred, New York.

MICROGRID WITH ELECTRIC VEHICLES

BY

BEHROUZ AZIMIAN

B.S. IRAN UNIVERSITY OF SCIENCE AND TECHNOLOGY (2016)

SIGNATURE OF AUTHOR \_\_\_\_\_

APPROVED BY \_\_\_\_\_

XINGWU WANG, ADVISOR

\_\_\_\_\_  
EHSAN GHOTBI, ADVISORY COMMITTEE

\_\_\_\_\_  
DAN LU, ADVISORY COMMITTEE

\_\_\_\_\_  
WALLACE B. LEIGH, CHAIR, ORAL THESIS DEFENSE

ACCEPTED BY \_\_\_\_\_

GABRIELLE G. GAUSTAD, DEAN  
KAZUO INAMORI SCHOOL OF ENGINEERING

## **ACKNOWLEDGMENTS**

I would like to express my gratitude to Dr. Xingwu Wang for his continued guidance throughout the span of this endeavor. To my committee members, Dr. Ehsan Ghotbi and Dr. Dan Lu, I give thanks for their assistance. I would like to offer my special thanks to Dr. Jalal Baghdadchi, Laura Grove, and Samantha Dannick for the knowledge they contributed. Finally, I would like to thank my parents, my brother and my best friends Mohammadreza Shirkhani and Shirin Yousefi for their moral support from thousands miles away.

# TABLE OF CONTENTS

	<b>Page</b>
<i>Acknowledgments</i> .....	<i>iii</i>
<i>Table of Contents</i> .....	<i>iv</i>
<i>List of Tables</i> .....	<i>v</i>
<i>List of Figures</i> .....	<i>vi</i>
<i>ABSTRACT</i> .....	<i>viii</i>
<b>I. Introduction</b> .....	<b>1</b>
<b>II. published results</b> .....	<b>3</b>
<b>A. Stackelberg Game Approach on Modeling of Supply Demand Behavior Considering BEV Uncertainty</b> .....	<b>4</b>
<b>B. Can Renewables Stimulate BEV Demands? - Technical Principles</b> .....	<b>19</b>
<b>C. Cloud Computing Based Real-Time Energy Management System with RNN-LSTM Wind Forecasting</b> .....	<b>35</b>
<b>III. Unpublished work</b> .....	<b>45</b>
<b>IV. Summary and Conclusions</b> .....	<b>55</b>
<b>V. Future Work</b> .....	<b>56</b>
<b>VI. References</b> .....	<b>57</b>

## LIST OF TABLES

	<b>Page</b>
Table II. A. I. Different Characteristics of BEVs .....	12
Table II. A. II. Satisfaction Function and Generation Coefficients .....	14
Table II. A. III. Numerical Performance Evaluation .....	17
Table II. A. IV. Statistical Results for Generation Values in [kw] .....	18
Table II. B. I. Assumed Characteristics of BEV .....	28
Table II. B. II. Energy Production and Consumption for Each Renewable Source and Demand for Expected Values of Random Variables .....	30
Table II. B. III. Summary f Number of BEVs and ESS For Normal and Power Outage Condition .....	33
Table II. C. I. Generation/Load Data .....	40
Table II. C. II. Generation of Different Components For Different Wind Speeds .....	41
Table II. C. III. Different Component Generation Status for Different Operation Mode .....	43

## LIST OF FIGURES

	<b>Page</b>
Figure II. A. 1. System model of the retailer company and users.....	7
Figure II. A. 2. Arrival time pdf for BEV owners in rural areas in New York State.....	11
Figure II. A. 3. Departure time pdf for BEV owners in rural areas in New York State ...	11
Figure II. A. 4. Average travelled distance pdf for BEV owners in rural areas in New York State.....	11
Figure II. A. 5. Required time to fully charge a BEV with respect to distance driven and car size.....	12
Figure II. A. 6. Stackelberg game theory algorithm .....	13
Figure II. A. 7. Load Profiles for Groups 2 and 3 of Consumers Before and After Applying Optimization Algorithm.....	15
Figure II. A. 8. Uncertain Load Profile of 50 BEVs Before Applying the Algorithm without V2G technology.....	15
Figure II. A. 9. Uncertain Load Profile of 50 BEVs After Applying the Algorithm with V2G technology.....	16
Figure II. A. 10. Load Profiles for Group 1 of Consumers Before and After Implementing the DR program .....	16
Figure II. A. 11. Aggregated Generation Profiles Before and After Applying Optimization the Algorithm.....	16
Figure II. A. 12. Conventional and Real-Time Prices Broadcasted by Retailer .....	17
Figure II. B. 1. 2014-2016 BEV sales volumes per 100 thousand people in 11 countries (Data are derived from Global EV Outlook 2017 and population in eachcountry.).....	20
Figure II. B. 2. Planned renewable power generations and EV battery storages.....	22
Figure II. B. 3. Load curve and multi-level step model.....	25

Figure II. B. 4. Expected hourly renewable power generations for solar (red line), wind (blue line) and biomass (green line).....	26
Figure II. B. 5. PDF of morning arrival time (A), evening arrival time (B) and travel distance (C) .....	28
Figure II. B. 6. Confidence interval of mean for BEV load profile with sample of size 275 over 24 hours .....	30
Figure II. B. 7. Hourly renewable power generation and battery discharging (left), load and battery charging(right), and operation mode for expected values of random variables.....	31
Figure II. C. 1. Standard RNN .....	36
Figure II. C. 2. RNN-LSTM .....	36
Figure II. C. 3. LSTM structure for wind power forecasting.....	37
Figure II. C. 4. Real-time testbed for microgrid studies along with IoT infrastructure for wind forecasting. ....	37
Figure II. C. 5. Wind power prediction along with actual wind power production.....	38
Figure II. C. 6. Microgrid testbed .....	39
Figure II. C. 7. Active power generation of different units. ....	41
Figure II. C. 8. Active power generation before and after of fault occurrence .....	42
Figure III. 1. PSS/E GUI environment for input data .....	46
Figure III. 2. Running power flow analysis from PSS/E GUI.....	47
Figure III. 3. 5 Bus system diagram with line flows.....	47
Figure III. 4. Excel file output for violation report .....	53
Figure III. 5. PSS/E power flow results for scaled up load at bus 150 .....	53

## **ABSTRACT**

The targeted goal of the renewable energy penetration level in New York State's electric power generation for 2030 is 50%. New wind farms are being proposed, planned and installed in upstate New York. The downstate region of New York (Long Island, New York City, and the Hudson Valley) uses 66% of the state's electric energy. While, its power plants generate only 53% of the state's electricity. There are two essential requirements: 1. Enabling upstate resources to better serve downstate consumers, and 2. Local consumptions with energy storages such as batteries in distribution network. One can envision a resilient power network to resist power outages due to extreme weather and other unexpected events. Forming a community power island may be beneficial to use some upstate wind power resources.

Alfred University is exploring the use of wind power generation of upstate New York along with photovoltaic and biomass generation to implement a microgrid in Alfred, NY. In this regard, the impact of battery electric vehicles is also investigated during normal and outage grid operation modes. In this modeling study, the microgrid operates in real time (i.e. milliseconds interval) or day-ahead scheduling (i.e. hourly interval). That is, renewable energy generation and battery storages are modeled in both time intervals and several simulations are conducted.

## I. INTRODUCTION

In recent years, number of electric vehicles (EVs) is increasing rapidly. The EV batteries may be programmed to have two-way communication with power grid. With the development of charging facilities, it is possible to send/receive power from electric vehicles. This feature could be utilized to dispatch energy back to the grid when there is an outage. The second hand batteries from old electric vehicles could also be employed to smooth the intermittent renewable energy generation.

By installing renewable energy units such as wind, solar, biomass in distribution network adjacent to consumers, small scale power systems can be formed called microgrid. The aim of this study is to examine the correlation between electric vehicles and renewable energy generation in a microgrid.

Generation and load are both exist in micrgrids and this could provide many opportunities for grid operators. For instance, during power outage conditions, islands can be formed to meet the load with minimum amount of load shedding. The main drawback of renewable energy is the intermittent nature of it. The most suggested viable practice is energy storage system. The interaction of electric vehicles and renewable energy could be a topic that has to be addressed because they will help to build the microgrids.

In the next sections, first, day ahead planning approach is considered to manage power grid, renewable energy generation and electric vehicles. We present an algorithm to smooth the impact of electric vehicle charging on power grid. In addition, the possibility of using the extra energy stored in electric vehicles battery is studied. After we propose the possible actions for managing electric vehicle charging challenge for current state of the grid operation, then the trend of electric vehicle purchases is investigated and the possible correlation between the number of electric vehicles being purchased in each year and renewable energy expansion plans is examined.

After possible corrective actions are determined for microgrid operation, the real time operation of the system needs to be studied. For this purpose, all the components of microgrid including extra renewable energy units, electric vehicles and transmission lines are simulated in real time simulator.

This study can be regarded as a comprehensive study of microgrid which could be used for future planning policies and energy management systems.

## II. PUBLISHED RESULTS

The following studies have been carried out in this thesis study and their results have been published/submitted in various papers and poster:

A) B. Azimian, R. F. Fijani, E. Ghotbi and X. Wang, "Stackelberg Game Approach on Modeling of Supply Demand Behavior Considering BEV Uncertainty," 2018 IEEE International Conference on Probabilistic Methods Applied to Power Systems (PMAPS), Boise, ID, 2018, pp. 1-6.

B) X. Li, B. Azimian, P. Chen, X. Wang, "Can renewables stimulate BEV demands? Technical principles and cross country empirical studies," 2019 IEEE Industry Applications Annual Meeting (IAS), Baltimore, MD, (Submitted)

C) B. Azimian, D. Lu, X. Wang, "Cloud Computing Based Real-Time Energy Management System with RNN-LSTM Wind Forecasting," 2018 IEEE Power and Energy Society General Meeting (PES GM), Portland, Or, 2018. (Poster)

The contents of these published manuscripts will be found in the following sections of this chapter.

## A. Stackelberg Game Approach on Modeling of Supply Demand Behavior Considering BEV Uncertainty

### Abstract

Based on advanced metering infrastructure (AMI), one can use big data to provide demand-response (DR) solutions. There is a need to develop optimized cost structures for consumers. In this paper, Stackelberg game approaches are utilized, and residential loads are considered including battery electric vehicles (BEVs) equipped with BEV communication controllers and vehicle-to-grid (V2G) technologies. Efficient and effective optimized algorithms are developed for users (followers) based on time dependent pricing schemes. In the “games,” besides the followers, other participant is an electricity retailer company (leader), with a two-way bilateral communication procedure accepted and established by all participants. The user side of the games is related to the demand side management (DSM). Real-time pricing (RTP) from time-of-use (TOU) companies is used to achieve better results. Monte Carlo simulations (MCS) represent uncertain behaviors of BEV drivers. Results indicate that customers’ demands can be met while reaching the best efficiency.

### I. Introduction

In a traditional power grid, proper metering may decrease demand response (DR) non-scheduled loads slightly. In a smart grid, several advanced techniques can be integrated, including advanced metering infrastructure, energy management systems, distributed energy systems, intelligent electronic devices, internet of things (IoTs), and battery electric vehicles (BEVs) [1]. When a smart metering infrastructure is combined with DR programs, efficiency can be improved [2]. Two types of DR have been discussed previously: 1. The retailer has all the power to directly control consumers’ usage which decreases the satisfaction of the users; and 2. The retailer reshapes DR programs through dynamic pricing such as critical pricing and real time pricing (RTP) [3]. The second type is preferred in this study.

Modern energy managements via smart grids may take advantages of following technology developments: bi-directional energy flows, price-responsive loads, intelligent electronic devices (IEDs), and phasor measurement units (PMUs). Thus, sophisticated

smart metering facilities and advanced two-ways communication technologies enable more flexible energy generations, deliveries and consumptions [4-7]. In a self-scheduling model simulation, consumers can participate “day-ahead” energy markets in order to minimize costs and/or maximize profits [8]. Price uncertainty was studied for generation company as a leader in game theory framework [9-10]. Recently, game theories are being considered in DR solutions and load peak shavings. In references [11-12], a Stackelberg game approach was used to deal with DR scheduling under load uncertainty based on real-time pricing in a power grid. In references [13-14], similar approaches were used to stimulate a power company and its customers to “play the game” in order to maximize their benefits and to eventually flatten aggregated load curves. With bi-level hybrid multi-objective evolutionary algorithms, utility companies’ profits may be optimized [15]. Additionally, various approaches have been developed to find the clearing price in retail electricity markets with high penetrations of renewable energies. Based on a time-of-use (TOU) pricing structure, providers or retailers can charge a calculable fee for the fixed price depending on an amount of consumption during a specific time interval [16-17]. Commonly, electric vehicles are connected to grids to receive energy, and limited savings can be achieved when charging schedules are adjusted to avoid peak load periods [18]. In a case study, benefits of the coordinated EV charging strategy were considered in terms of energy cost savings and peak-to average ratio reductions [19]. An autonomous energy management system was used to allow residential users selling energy back to the utility company by discharging the PEV’s battery [20]. An optimization approach was suggested to provide an optimal charging strategy for the EVs to proactively control their charging speed to minimize the cost of charging [21]. An online electric vehicle scheme was considered to provide electric power to the vehicle wirelessly by a smart grid [22]. With a power payment function, the smart grid can maximize the social welfare of the online electric vehicle’s needs.

Using Stackelberg game theory approach, performance can be substantially improved with a demand response program [3]. To our best knowledge, there is no literature in public domain to systematically consider electric vehicle owner’s driving behaviors via the game theory. In this study, a mixed integer nonlinear programming scheme is considered to achieve benefits for both “energy providers” and “consumers.” A

new approach is considered here to flatten peak loads by scheduling home appliances and BEVs which can be charged and discharged via two-way technologies by combing grid-to-vehicle (G2V) and vehicle-to-grid (V2G) connectivity. By using V2G technologies, retailers can buy energy from consumers if such practices are mutually beneficial. Thus, the following sections will study advanced two-way communication links and BEVs charging/discharging schedules to maximum utility companies' profits via peak-shaving, and to satisfy consumers by elevating their roles to participants and to minimizing costs. Using a price-based model to guarantee an efficient algorithm between an electricity retailer and users owning BEVs with the aim of balancing the load. Main contributions of this paper include following key points:

- Using a price-based model to develop an efficient algorithm between retailers and users (with BEVs), and aiming for balanced supply-load by shaving peaks;
- Generating optimized results for both retailers and users with an iterative algorithm, and finding Stackelberg equilibrium (SE) to achieve optimal loads for both parties;
- Formulating 1-N leader-follower Stackelberg relationship between one retailer and  $N$  users; and adopting the RTP function of the retailer and the utility function of  $N$  users; and
- Handling uncertainty of different driving habits of BEV owners by MCS.

Specifically, the rest of the paper is organized as follows. Section II discusses the system model and formulates the Stackelberg game theory. In Section III, we use data to generate load profiles of BEVs. Some key aspects of Stackelberg game theory and the logic are presented in Section IV. Results are provided in Section IV, and conclusions are drawn in Section V.

## II. SYSTEM MODEL

In Fig. II. A. 1, a model is established for one utility company and  $N$  users with BEVs. These users will adjust their electricity usages by using advanced metering infrastructure and heterogeneous communication technologies, with the ultimate goals to reduce overall costs. The utility company (retailer) can provide hourly price structures to these users to encourage peak shaving and ultimately to maximize profits.

Advanced communication technologies enable the cloud computing environment and real time sensing/controlling including IoTs [23]. In this environment, an entity represents an electric load (consumer) or a prosumer such as a BEV. In the cloud environment, the real-time access to each entity is guaranteed. The system operator can categorize users into different groups. As shown in Fig. II. A. 1, all prosumers can be placed in one group, and other conventional loads in other. By utilizing instantaneous two-way communication links, real-time electricity prices will be broadcasted, conventional users' consumption behaviors will be adjusted, and BEVs charging/discharging schedules can be changed. To maintain system stabilities and guarantee maximum profits, the retailer can impose load curtailment during peak hours.

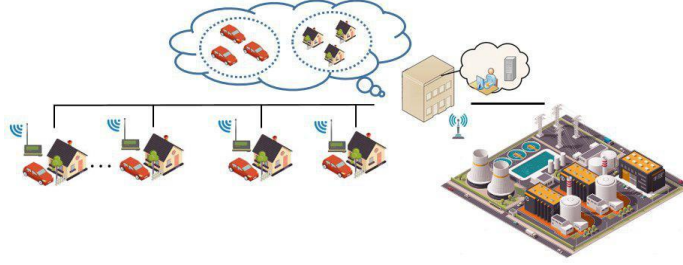


Figure II. A. 1. System model of the retailer company and users

#### A. Retailer Company Model

In this model, the cost function for the retailer is labelled as  $C_t(g_t)$ , and depends on the amount of electricity provided ( $g_t$ ) during an interval  $t$ ; where  $t \in T, T = |T|$  that is a strictly convex and monotonically increasing function.

$$C_t(g_t) = \frac{a_t}{2} g_t^2 + b_t g_t + c_t \quad (1)$$

Where  $a_t, b_t$  and  $c_t$  are the generating coefficients. During different time intervals, each coefficient has a different value.

Taking a differential operation against (1), one obtains the marginal cost function  $C'_t$ :

$$C'_t(g_t) = a_t g_t + b_t \quad (2)$$

which is the cost to produce one more unit of electricity. Such marginal cost must be lower than the actual cost in order to guarantee profits for the retailer company. So, market price equation can be defined:

$$P_t(g_t) = \lambda_t C'_t(g_t) = \lambda_t(a_t g_t + b_t) \quad , \quad \lambda_t \geq 1 \quad (3)$$

where  $P_t$  is price at each time slot and  $\lambda_t$  is a time-wise profit coefficient. In reference [15], a similar profit coefficient was introduced, minimized and validated. In this paper, there are 24 time intervals (slots), corresponding to 24 prices in a day. The retailer provides electricity and its price to the consumers who will decide how much to use in each time interval. Thus, a user can move his/her electricity usages to off-peak intervals to minimize the total costs. The retailer wants the most profit and the least aggregated peak load in order to avoid expensive backup generators. Flattening the demand load should be two-ways as a user has critical needs for electricity. To determine the optimal generation vector, one should minimize variations in generation, and match supply with demand. Therefore, the retailer problem can be formulated as follows:

$$\min \quad U_{RC}(g_t) = \sum_{t \in T} (g_t - \bar{g})^2 \quad (4)$$

$$\text{s.t.} \quad L_t \leq g_t \leq \min(g_t^+, L_t^{\max}) \quad (5)$$

$$L_t = \sum_{n=1}^N l_{n,t} \quad (6)$$

$$L_t = \sum_{i=1}^{N-1} l_{i,t} + l_{n,t} \quad i \neq n \quad (7)$$

Where  $U_{RC}$  is the utility function of the retailer company and  $\bar{g}$  is an average power generation during a day.  $L_t$  is the summation of electricity demands of all  $N$  users during the time interval  $t$ .  $g_t^+$  is the maximum capacity of the retailer company's generation at the interval  $t$ ,  $L_t^{\max}$  is the overall upper bound of the total power demands for slot  $t$ .  $l_{n,t}$  is the power consumed by user  $n$  in the interval  $t$ . One must notice that the above-mentioned function is different from profit maximization. In (4), minimizing utility function may lead to maximized profits. In (5), the generation should always meet the total demand of all users, and be lower than the smallest threshold for generation capacity and upper load ranges. In (6) and (7),  $L_t$  can be obtained by asynchronous user's adjustment of consumption, reflecting the human nature that no two users will react to real-time pricing schemes due to different needs. In (7), a user adjusts his/her usage, while others don't. In

such non-simultaneous framework, no two users will negate their effects by increasing and decreasing their demands at the same time.

### B. User Model

Each user has its own utility function, shown in (8). According to what has been explained in Section II, with the application of IoTs, the user can be an entity representing an electric load (consumer) as the first term, or a prosumer such as a BEV as the second term. Function  $\psi_{n,t}(x_{n,t})$  models the satisfaction of the electricity consumers; in which  $x_{n,t}$  is the general power consumption variable,  $l_{n,t}$  being the residential demand and  $s_{n,t}$  being BEV demand. The third term is the total amount of money to be paid by the consumers, which leads to less satisfaction as represented by a negative sign. With this, the demand side problem is formulated as follows:

$$l, s = \arg \max U_n(l_n, s_n) = \sum_{t=1}^{24} \psi_{n,t}(l_{n,t}) + \sum_{t=1}^{24} \psi_{n,t}(s_{n,t} \cdot P_n^{BEV}) - \sum_{t=1}^{24} P_t(g_t) \cdot (l_{n,t} + s_{n,t} \cdot P_n^{BEV}) \quad (8)$$

$$\psi_{n,t}(x_{n,t}) = \omega_{n,t} x_{n,t} - \frac{\theta_n}{2} x_{n,t}^2, \quad \omega_{n,t} > 0 \quad \theta_n > 0 \quad (9)$$

$$\text{s.t. } l_{n,t}^- \leq l_{n,t} \leq l_{n,t}^+ \quad (10)$$

$$\sum_{t=1}^{24} l_{n,t} = L_n \quad (11)$$

$$\sum_{t=1}^{24} s_{n,t} = T_n^{req} \quad (12)$$

$$\sum_{t=1}^{24} |s_{n,t}| \leq T_n^{\max} \quad (13)$$

$$SOC_{n,T}^{dep} = BC_n \quad (14)$$

where  $\omega_{n,t}$  is the preference parameter with indices  $n$  (user) and  $t$  (time),  $\theta_n$  is a predetermined constant integer,  $L_n$  is the total daily energy usage,  $s_{n,t} \in \{-1, 0, 1\}$  is a discrete variable which is multiplied by rated battery power  $P^{BEV}$  of electric vehicles and indicates BEV charging  $\{1\}$ , discharging  $\{-1\}$  status. If it is charging, it will have a positive effect on satisfaction of the utility function, and if it is discharging, it has a negative effect. Although discharging has a negative effect on satisfaction, it is losing the power obtained in the past charging periods. However, by selling discharged electricity, it has positive

effect on the third term of utility function.  $T_n^{req}$  is the required time to fully charge the BEV,  $T_n^{max}$  is the maximum number of hours that the battery is interacting actively with the network,  $SOC_{n,T^{dep}}$  shows the BEV state of charge, and  $BC_n$  is the battery capacity,  $T^{dep}$  is the vehicle's departure time from the house. (9) Denotes the satisfaction function  $\psi_{n,t}(x_{n,t})$  of the user  $n$  by consuming  $l_{n,t}$  amount of electricity. (10) provides the upper and lower boundaries for electricity demand of  $n^{\text{th}}$  user  $n$  for interval  $t$ . (11) expresses the temporally-coupled constraint which wouldn't reduce the total daily consumption of the user  $n$ , so we can apply load shedding only in terms of pick shaving and load shifting. (12) states the cumulative charging time in order to fully charge the BEV before leaving one's residence. (13) limits the maximum number of hours for a BEV connected to the grid system, either in G2V or V2G mode. Therefore, by limiting the hours that the battery is being charged or discharged, we reduce the detrimental effect of constant battery usage. In (14) the sequence of charging/discharging should be in a way that by the time that the BEV owner decides to leaves the house, the SOC should be 100%.

In the Stackelberg equilibrium context and the hierarchical process, our aim is to maximize the leader's (retailer) utility function by having the data of the follower's (user) rational reaction set (RRS). The existence of the Stackelberg equilibrium has been discussed and shown in [4]. In addition, the model in (8) is formulated as a mixed integer nonlinear programming problem, and can be solved via MATLAB-GAMS interface.

### III. BEV LOAD PROFILE

To model BEV load profiles, data from National Household Travel Survey (NHTS) for rural New York State were utilized to estimate average driving mileages and optimize battery usages. The SOC of the vehicles upon their home arrival time is of crucial importance [24]. Table II. A. I shows the data according to different types of cars and different characteristics. Also, in Figs. II. A. 2-4, probability distribution functions (PDFs) for driving behavior, including arrival time, departure time, and traveled distance in rural areas in New York state has been drawn from NHTS data. The reason why we chose rural areas in New York State is that Alfred University is located in rural areas.

Moreover, configuring the time of fully charged BEV depends on the distance it travels daily, and we assume that BEV is a constant power prosumer. From Fig. II. A. 2, we obtain the required charging time based on daily driven distance [25-26].

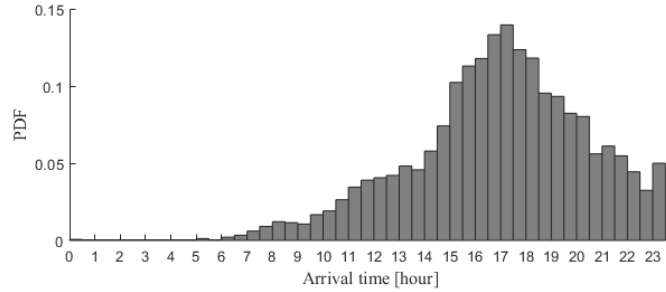


Figure II. A. 3. Arrival time pdf for BEV owners in rural areas in New York State

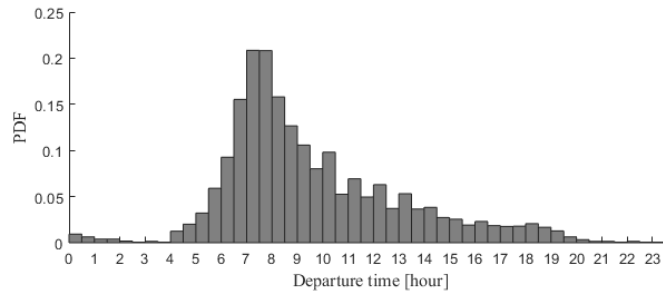


Figure II. A. 4. Departure time pdf for BEV owners in rural areas in New York State

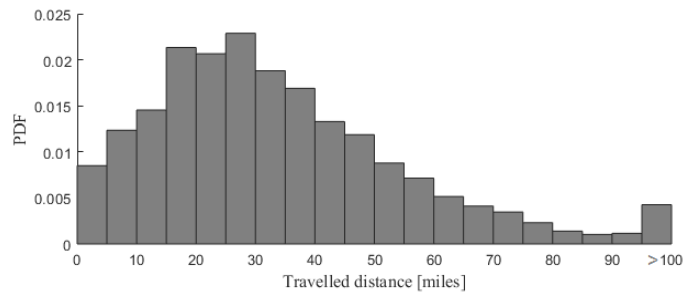


Figure II. A. 5. Average travelled distance pdf for BEV owners in rural areas in New York State

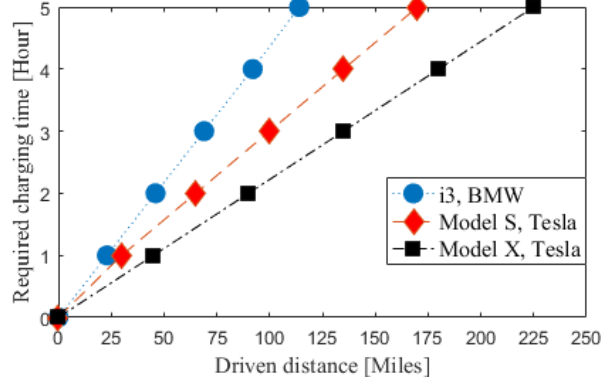


Figure II. A. 6. Required time to fully charge a BEV with respect to distance driven and car size

Table II. A. I. Different Characteristics of BEVs

Vehicle Type	Commercial model	Expected Market Share [%]	Energy [kW-hr]	Rated Battery Power [kW]	Single Charge Drive-Range [mile]
Compact sedan	i3, BMW	51.48	33	7	114
Mid-size sedan	Model S, Tesla	10.35	75	11.5	259
Mid-size SUV	Model X, Tesla	38.17	100	17.2	295

#### IV. STACKELBERG GAME THEORY ALGORITHM

In Fig. II. A. 6, iterative DR algorithm is illustrated via a flow chart. At the beginning of the computation, the retailer broadcasts hourly price one hour ahead. According to (3), marginal cost function is calculated by power generation requirement and initial price broadcasted. As the relationship between the price equation and power is linear, the algorithm uses the generation value. Final prices can be found once the total power generation value is known. Afterwards, Monte Carlo simulation emulates driving behaviors of BEV owners.

Users respond to the prices broadcasted, and shift their usages to non-peak time slots. BEV discharging features can help the retailer company to offset some loads during peak hours. The peak-shaving and the demand aggregation can be accomplished continuously instead.

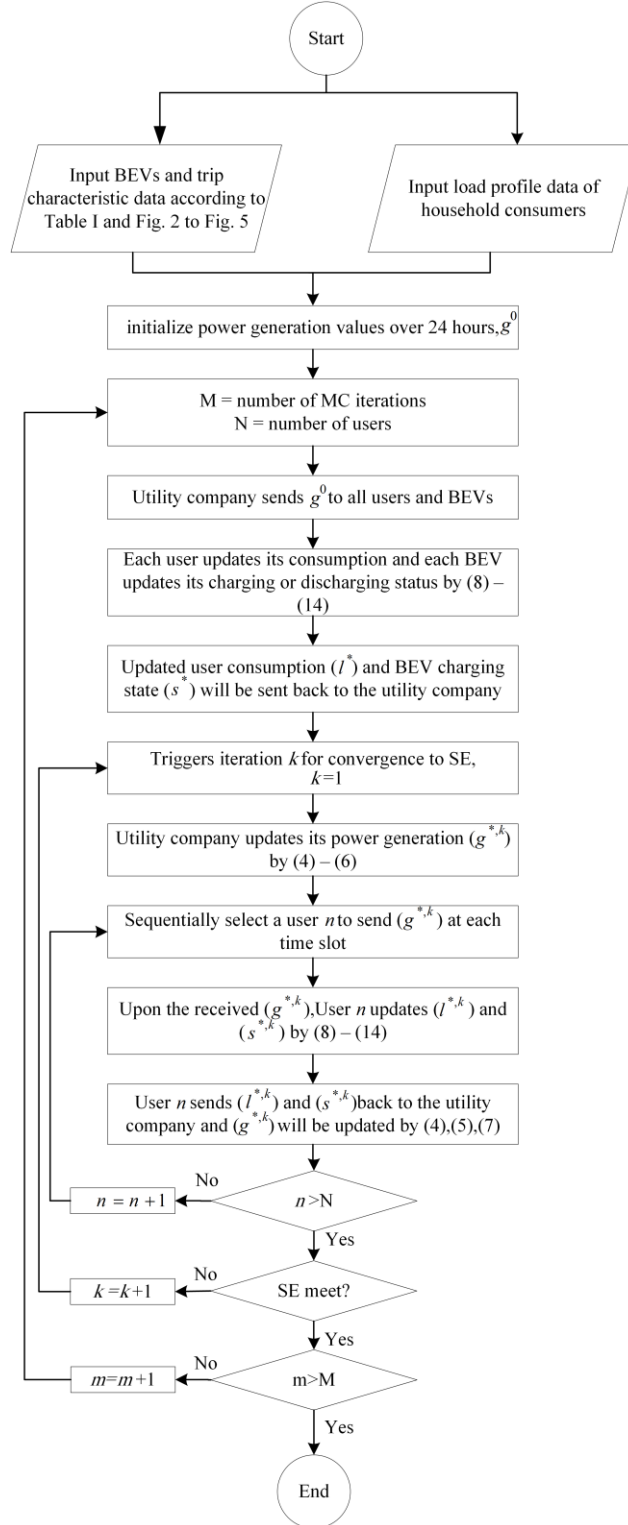


Figure II. A. 7. Stackelberg game theory algorithm

## V. SIMULATION AND RESULTS

Residential consumers are divided into three groups as tabulated in Table II. A. II. Group 1 corresponds to utility function coefficient  $\omega_{n,t}$  of 5.0, with 50 BEVs. Groups 2 and 3 do not have BEVs, but have different utility coefficients. The minimum and the maximum values refer to the lower and upper bounds of the targeted power demands. For example, Group 1 consumption varies between 70% and 150% of its nominal load. The price coefficient is kept constant, i.e.,  $\lambda_t = 1.2$ . In Fig. II. A. 8, load profiles are shown for Group 2 and 3; and benefits from the game theory applications can be visualized by examining a profile with or without the algorithm. In general, the load profiles are flattened due to users' participations. In comparison with Group 2, Group 3 shows less eagerness to participate as it has larger  $\omega_{n,t}$ . For group 1, as illustrated in Table II. A. II, managing the vehicle's V2G or G2V status is of great importance.

Table II. A. II. Satisfaction Function and Generation Coefficients

Group	Utility function coeff.		Generation Coeff.		Min Demand %	Max Demand%
	$\omega_{n,t}$	$\theta_n$	$a_t$	$b_t$		
1	5.0	0.1	0.01	0.2	70	150
2	5.5	0.1	(00:00-8:00)		75	140
3	6.0	0.1	(8:00-24:00)		80	120

If a large number of BEV owners begin to charge their vehicles immediately returning home, the sudden power load may be undesirable. By applying the algorithm in Fig. II. A. 9, the uncertainty related to random behaviors of BEV owners can be managed by optimizing charging and discharging activities. In Fig. II. A. 8, wide bands of load profile for BEVs are shown for each time slot in a day. Without game theory applications, the users' peak load can coincide with that of the BEV charging peaks. In Fig. II. A. 9, modified BEV load profile is obtained after applying the algorithm. The negative values represent the V2G feature of the BEVs, or discharging. After coming back to home (between 17:00 or so and midnight), most vehicles are either sending back power to the grid or in standing by mode. The charging period mainly happens between 1:00 and 6:00.

Comparing the time interval between 14:00 to 16:00 in Fig. II. A. 7 and Fig. II. A. 10, more peak shaving has been achieved for

Group 1 due to the presence of V2G technology. Fig. II. A. 11 shows the total generation over 24 hours for users' aggregated demand with and without implementing the DR program. The expected value at each hour is used to obtain the profiles in Fig. II. A. 10 and Fig. II. A. 11. From Table II. A. IV, the standard deviation shows that more fluctuations will happen mainly from 22:00 to 24:00 and 1:00 to 5:00. Therefore, the power system operator should consider more spinning reserve after midnight; this will cause an increase in power system operation cost. Finally, the real-time prices over 24 hours that has been derived from the algorithm is compared with the conventional price in Fig. II. A. 12. The performance of the algorithm is evaluated by two scenarios (with and without RTP and V2G) from various aspects.

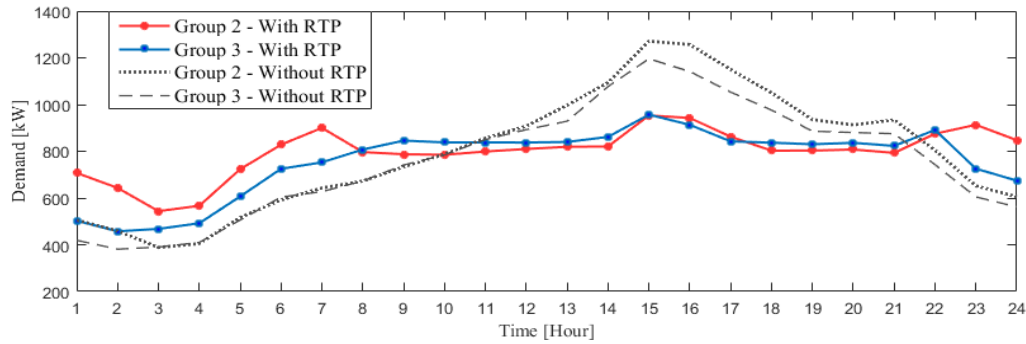


Figure II. A. 10. Load profiles for groups 2 and 3 of consumers before and after applying optimization algorithm

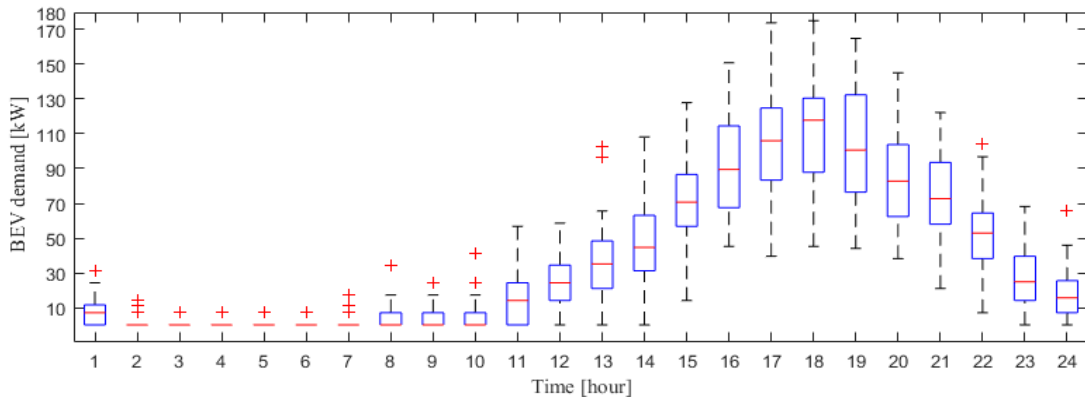


Figure II. A. 11. Uncertain load profile of 50 BEVs before applying the algorithm without V2G technology

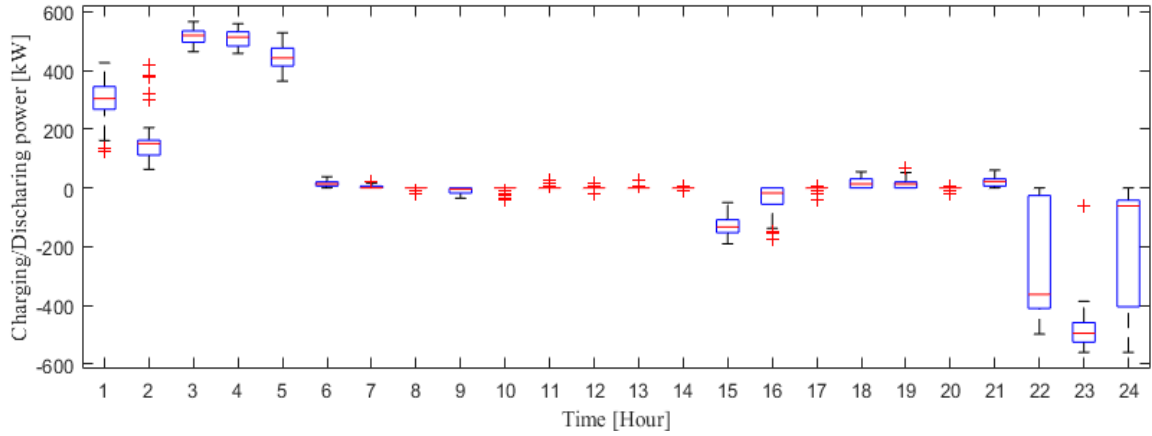


Figure II. A. 12. Uncertain load profile of 50 BEVs after applying the algorithm with V2G technology

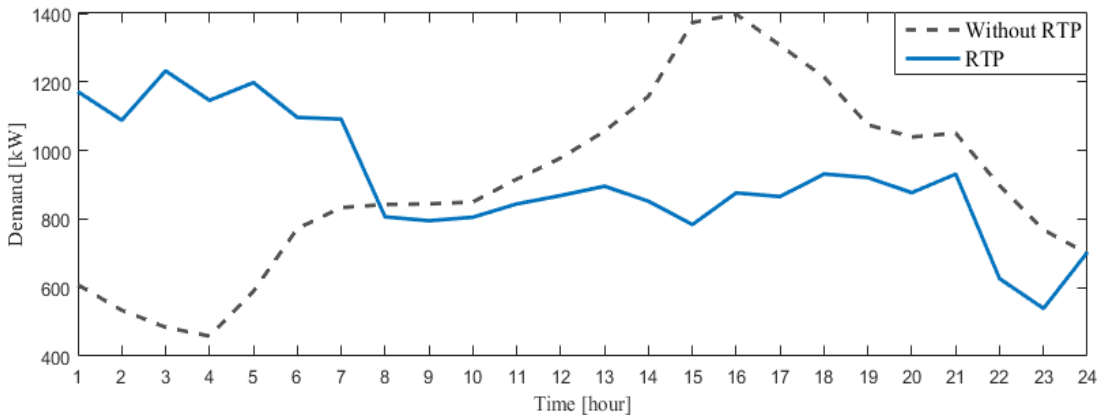


Figure II. A. 13. Load profiles for group 1 of consumers before and after implementing the DR program

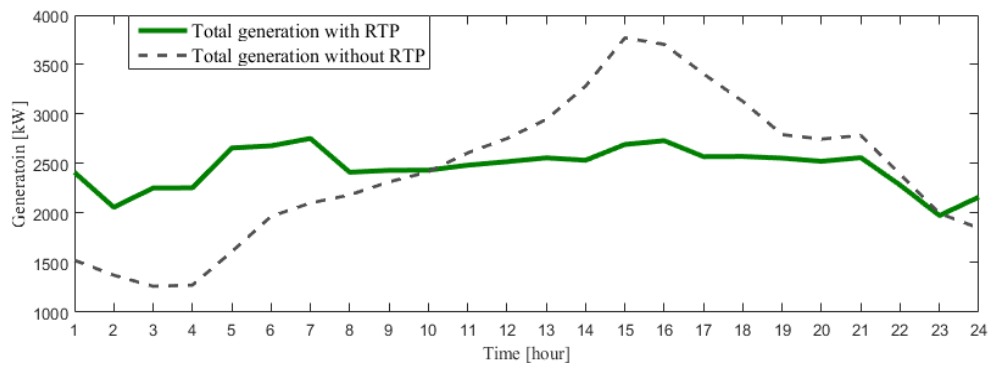


Figure II. A. 14. Aggregated generation profiles before and after applying optimization the algorithm

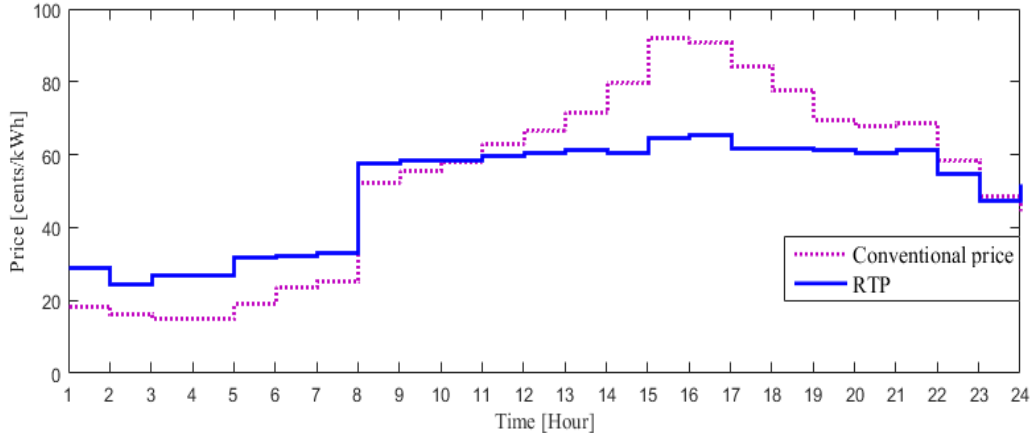


Figure II. A. 15. Conventional and real-time prices broadcasted by retailer

The numerical results are shown in Table II. A. III. The peak demand is significantly decreased by almost 1 MW. Total energy usage has not been changed, which proves that the retailer cannot reduce the whole amount of energy that a user expects to consume per day. This reality is shown in (11). Using algorithm in Fig. II. A. 6, the total user payments decreased about 16%, which demonstrates the efficiency of game theory application. Additionally, the generation costs of both scenarios can be less than the total payments, i.e., making profits for the retailer.

Table II. A. III. Numerical Performance Evaluation

Scenario	Peak demand [kw]	Total Energy Usage [kwh]	Total Payments [\$]	Generation Cost [\$]
Without RTP and Without V2G	3841	59092	36135	15115
RTP and V2G	2755	59092	30244	12661

Table II. A. IV. Statistical Results for Generation Values in [kw]

Time [hour]	1	2	3	4	5	15	16	17
$g_t$ Expected value	2412	2060	2255	2256	2659	2694	2732	2571
$g_t$ Standard deviation	66	76	26	28	42	29	49	12
Time [hour]	18	19	20	21	22	23	24	
$g_t$ Expected value	2573	2556	2524	2561	2283	1976	2163	
$g_t$ Standard deviation	14	14	8	16	130	66	197	

## CONCLUSION

Using game theory algorithm, one can reduce costs to consumers and potentially reshape generating profiles. In this paper, a model included one retailer and N users (with some of them owning BEVs). In particular, an optimized approach can shave peaks with DR managements. The game theory and Stackelberg equilibrium have been utilized to illustrate an algorithm for three different user groups. By comparing the results with and without DR managements, the efficiency of the algorithm can be shown. Using MCS in MATLAB-GAMS, the stochastic behavior of BEVs are simulated. According to the statistical analysis, such algorithm based on the game theory can reduce the peak loads. We are currently investigating possibilities to include more leaders and followers as well as incorporating solar and wind energy.

## **B. Can Renewables Stimulate BEV Demands? - Technical Principles**

### **Abstract**

Renewables and BEVs may potentially reduce environmental pollutions and traditional energy consumptions. However, existing literature does not study them holistically, combining technology with economy. In this paper, we first examine complimentary nature of these two technologies in a New York State college. Then, we establish an econometric model to study impacts on BEV demands due to renewables and five other socioeconomic factors, using 2010-2016 panel data from eleven countries. After multi-linear regressions, we observe that renewables impact BEV demands positively; i.e., one percent increment in renewables would yield 2% increment in BEV demands per 100 thousand people. High gasoline prices may lead to high BEV demands. The number of chargers impacts BEV demands positively. Population density does impact BEV demands positively, as well as education levels. The elasticity for GDP per capita is larger than one. Finally, we make recommendations to decision makers to synergistically promote renewables and BEVs. Planners should properly select locations encompassing renewables, chargers, parking facilities, highway rest areas, shopping centers and community activity centers.

### **I. INTRODUCTION**

Environmental pollutions and traditional energy consumptions are two critical issues facing the entire world. Transportation consumes approximately twenty five percent of the total energy worldwide [27]. Correspondingly, the CO<sub>2</sub> emission from transportation accounts for nearly twenty three percent of the total emission [28]. To reduce local pollutions, many urban areas are considering new plans/policies to replace gasoline/diesel vehicles with Electric Vehicles (EVs) [29], [30]. There are two types of EV technologies: Plug-in Hybrid EV (PHEV) and Battery EV (BEV). The former uses fuels, while the latter does not. Recently, BEV's developments and deployments become more relevant to urban planners [31]. In Fig. II. B. 1, annual BEV sales volume density is illustrated for 2014-2016 [32]. Among eleven countries, Norway had the largest BEV density, and the highest percentage of renewables in electricity productions [33].

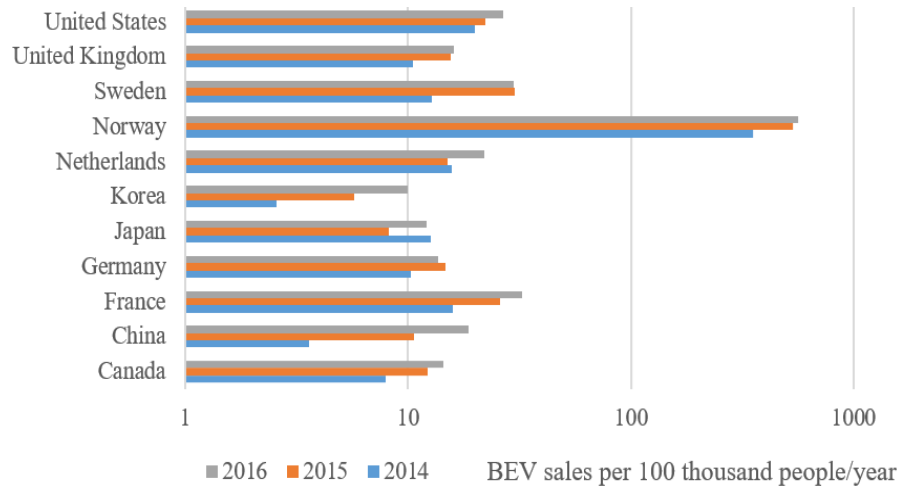


Figure II. B. 1. 2014-2016 BEV sales volumes per 100 thousand people in 11 countries (Data are derived from Global EV Outlook 2017 and population in each country.)

Renewables can reduce environmental pollutions and traditional energy consumptions. The percentage of renewables in world electricity production is approximately 24.5%, while that of coal is still around 40% [34], [35]. As the fastest growing renewable sources in the past decade, solar or wind power suffers from intermittent nature, which slows down the further penetration in electricity generations. The intermittency problems can be solved with appropriate storage devices such as batteries [36]. With BEV batteries, two different approaches have been proposed: 1. “spent” batteries retired from BEVs being utilized in a storage bank, and 2. BEVs being connected to smart grid systems via “Vehicle-to-Grid (V2G)” or “Grid-to-Vehicle (G2V)” schemes [37], [38]. To reduce traditional energy consumptions and pollutions globally, renewables and BEVs should be developed together, rather than two different funding sources and policy incentives. Electricity for BEV battery charging should come from renewables, and entire life cycles of BEVs can have very small negative impacts on the environment [39]–[44]. According to survey studies, BEV consumers want to charge batteries with electricity produced by renewables because environment performance is more important than price-value and range-confidence [45], [46]. One study predicted 23% increase in demands if electricity is from renewables [47]. Furthermore, if battery charging and discharging schedules match with electricity cost structures, BEV usage costs can be reduced; i.e., BEV owners can charge batteries during grid off-peak hours with cheap electricity, and “sell” stored electricity to offset peak loads for the grid.

Existing literature does not study renewables and BEVs holistically, combining technology with economy. As stated, previous studies were mainly based on surveys at the micro-economy levels. Using the newest cross-country data, this paper examines relationships between BEV demands and renewables, technically and economically. The remainder of the paper is arranged as follows. In Section II, an example is provided to explain such relationships technically. In Section III, an econometric model is established; using the BEV demand as a dependent variable, and renewables/socioeconomic-factors as independent variables and in subsection C, regression results are presented and explained. In Section IV, conclusions are drawn, along with suggestions to decision makers.

## II. RENEWABLES AND BEVs

When electrical energy from renewables is stored in batteries, synergetic relationships between renewables and BEVs can be shown technically. For this study, we'll consider eleven countries: Canada, China, France, Germany, Japan, Netherlands, Norway, South Korea, Sweden, United Kingdom and United States. Sample college/university campus can be found in each country due to following reasons: 1. Electric power grid systems on such campus only have a few feeders from utilities; 2. Reducing traditional energy usage is an integral part of education [48]. In this section, synergies are illustrated by using an example in New York State. Such principles can be utilized in other parts of the world.

For a rural area college in Western New York, we examined its daily electrical power load profile,  $P_{College\ load}(t)$  in January; and fitted it as follows:

$$P_{College\ load}(t) = 800 + 157\sin[(t - 9)(2\pi/T)] \quad (1)$$

where variable  $t$  is the time in hours, and period  $T$  is 24 hours. Load profiles were from New York State Gas and Electric (NYSEG) on line monitoring data for New York State College of Ceramics. Load profiles for other months are similar in curve fittings. The month of January is selected because it is the most important month for two reasons: 1. Cold weather, and 2. Beginning of new semester with students/faculty/staff returning to the campus. The average power is 800 kW, with the minimum of 643 kW and maximum of 957 kW. Typically, classes start at 9:00 and end at 21:00. Daily load profiles between

February and December are close to that illustrated in (1). Thus, this equation can be used in a model to represent daily power consumption each year. To accommodate such load profile, one can consider renewable energy sources and BEV battery storages. Using historical/local weather data and statistical predictions, hourly renewable power generations and battery storages should be able to carry the loads represented in (1). In Fig. II. B. 2, a college power island is illustrated for planned power generations such as wind (first generator on the right) solar (second generator on the right), and biomass (third generator on the right). Renewable energy models are documented in [49], [50] and detailed formulation is presented here because in our work, emphasis is given to BEV problem formulation rather than modeling different types of renewable energy units. Additionally, two storage systems are also shown including BEVs and Energy Storage Systems (ESS). Such island is desirable if there is a regional power outage, or if utility rates become extremely high due to peak load surcharges.

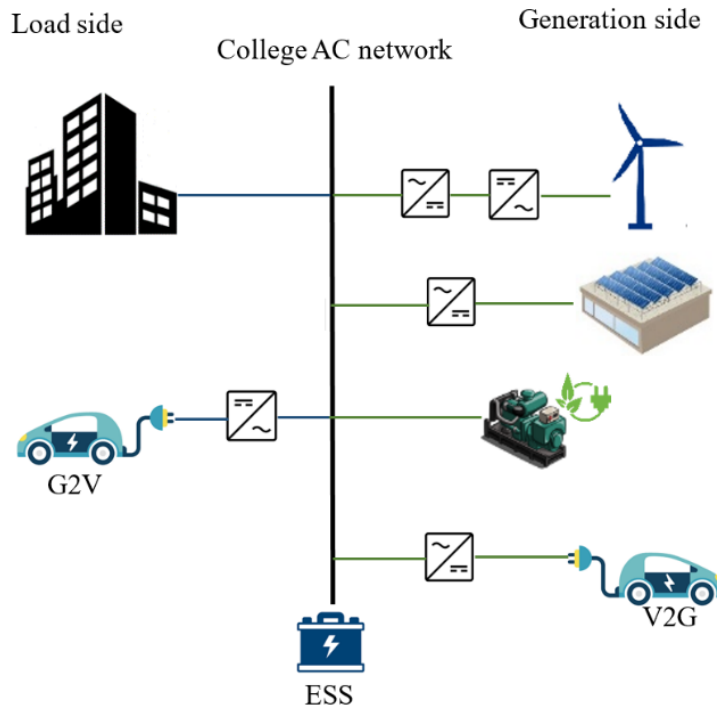


Figure II. B. 2. Planned renewable power generations and EV battery storages

There are different types of battery storage calculation models. In principle, the total renewable energy generations should exceed the total load energy demands on the

daily basis. When the renewable power generations are lower than the load power demands, the EV battery storage systems should provide the necessary power to the load if a power island is needed as shown in Fig. II. B. 2. To find the required ESS capacity, deterministic and non-deterministic approaches are utilized.

#### A. Deterministic Approach (DA)

For DA, all expected values for renewable generations, BEVs and loads are calculated by their probability distribution functions without considering uncertainties, for each given time slot such as one hour. For batteries, the State of Charge (SOC) is an important parameter, which has minimum and maximum values as boundaries as illustrated in (2) [51].

$$SOC_{min} \leq SOC \leq SOC_{max} \quad (2)$$

Commonly,  $SOC_{min}$  and  $SOC_{max}$  are equal to 40% and 100%, respectively. To estimate the ESS capacities, one examines the difference between power generations and demands for a given time slot such as each hour, as illustrated in (3).

$$\Delta P = P_{gen} - P_{dem} \quad (3)$$

Positive  $\Delta P$  indicates the generation surplus which can be used to charge the batteries, and negative  $\Delta P$  indicates generation deficiency which can be compensated by battery discharging. To balance generations with the demands for a given time slot, the curve of  $\Delta P$  versus time must have an average of zero over the same time. The energy curve can be obtained by integrating  $\Delta P$ . Thus, the difference between daily energy generations and demands is shown in (4).

$$\Delta W = \int \Delta P dt = W_{gen} - W_{dem} \quad (4)$$

Therefore, (4) can be used as a guide line to find the required storage capacity for the system illustrated in Fig. II. B. 2. Usually, a storage capacity parameter is defined by (5).

$$Essential \ storage \ capacity = Max \int \Delta P dt - Min \int \Delta P dt \quad (5)$$

If the total efficiency of the batteries and DC-AC inversions is  $\eta$  and batteries are limited to cycle between SOC 40% and 100%, the required storage capacity can be found by using (5) and  $\eta$ , as shown below.

$$\text{Required storage capacity} \geq \frac{\text{Essential Storage Capacity}}{0.6 \times \eta} \quad (6)$$

### B. Non-Deterministic Approach (NDA)

For NDA, to capture the uncertainties of solar/wind power generations and BEV owner's driving habits, a state sampling method is utilized in which every power state is selected. (Please note that biomass power generations will meet their expected values due to small fluctuations in feedstock such as wood chips.) That is, an available generation capacity is determined by its state, and total system generation capacity can be obtained by summarizing all generation capacities.

$$\text{Total renewable generation} = \sum_{j=1}^m G_{jk} \quad (7)$$

where  $G_{j,k}$  is the available capacity of the  $j$ th renewable generation unit in the  $k$ th sampling and  $m$  is the number of renewable generation units including wind, solar and biomass in the system.

Additionally, the load curve is represented by a multi-level step model as illustrated in Fig. II. B. 3. At each given step, the load value is assumed as an average value and the load uncertainty behaves as a normally distributed random variable.

For a given load level, a quantity called “the Demand Not Supplied” ( $DNS$ ) in the  $k$ th sampling is defined in (8).

$$DNS_k = \max \left\{ 0, L_i - \sum_{j=1}^m G_{jk} \right\} \quad (8)$$

where  $L_i$  is the total load at the  $i$ th level including college and BEV demands. If  $L_i$  is treated as a mean value, a standard deviation  $\sigma_i$  can be introduced and a normal distribution random number  $X_k$  can be used [52]. The sampled value of the load in the  $k$ th sampling is therefore given by (9).

$$L_{\sigma i} = (X_k \sigma_i + 1)L_i \quad (9)$$

To capture load uncertainty,  $L_{\sigma i}$  in (9) replaces  $L_i$  in (8). Loss of energy expectation (LOEE) can be found by two summations in (10).

$$LOEE = \sum_{i=1}^{N_L} \left( \frac{T_i}{N_i} \sum_{k=1}^{N_i} DNS_k \right) \quad (10)$$

where  $N_L$  is the number of the load levels in the multiple step load model shown in Fig. 3,  $T_i$  is the time length of the  $i$ th load level, and  $N_i$  is the number of samples at the  $i$ th load level. The unit of LOEE is MWh for a time period ( $T$ ) such as one day in this study. Considering the uncertainties of loads and renewable power generations and the battery SOC constraints in (2), the required storage capacity based on the NDA can be found below.

$$\text{Required storage capacity by NDA} \geq \frac{LOEE}{0.6 \times \eta} \quad (11)$$

where  $\eta$  is the total efficiency as described between (5) and (6).

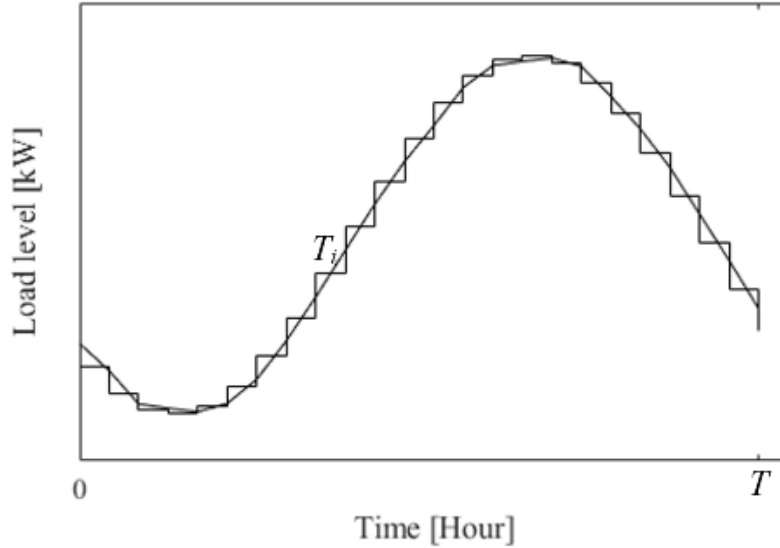


Figure II. B. 3. Load curve and multi-level step model

### C. System Data

Referring to Fig. II. B. 2 (upper left) and (1), the average load is approximately 800 kW. Three renewable power generations are illustrated on the right-hand side of the Fig.

II. B. 2. There is a considerable difference between the installed (nameplate) capacity and the actual output from a renewable energy system. Usually, the capacity factor is defined to illustrate expected output power over a long period, which is the ratio of actual energy generated over a time period (typically a year) to the maximum possible energy output over the same period. In Western New York, the capacity factor of solar and wind generation is 10% and 24%, respectively. In this study, the maximum power for wind (or solar) is 2 MW due to intermittency, and that for biomass is 400 kW. There are two types of EV batteries: a. BEV batteries with power of 7.4, 11.5 and/or 17.2 kW; and b. Battery ESS. In Fig. II. B. 4, projected hourly renewable power generations are illustrated for solar, wind and biomass based on historical data and probability calculations [53]. Please note that the projected wind (or solar) power generations in Fig. II. B. 4 are much lower than the planned maximum power capacities (2 MW).

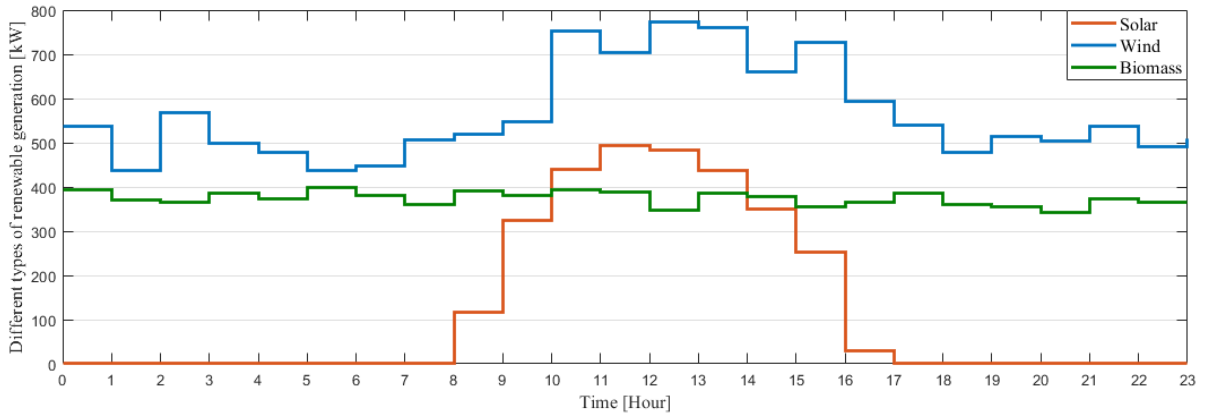
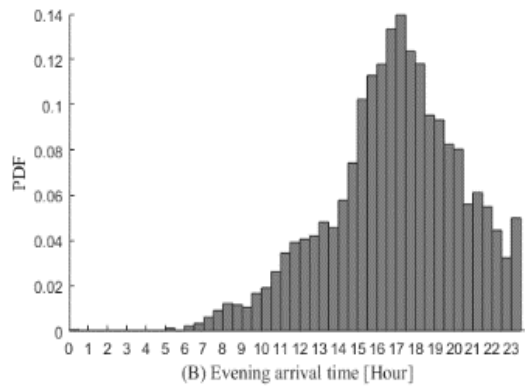
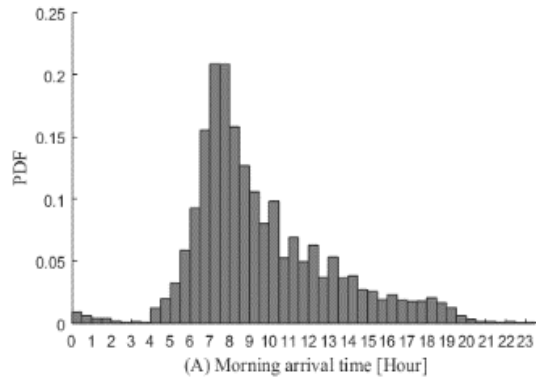


Figure II. B. 4. Expected hourly renewable power generations for solar (red line), wind (blue line) and biomass (green line)

Using DA, the lowest energy value is approximately 7.4 kWh for 8:00 time slot as the renewable generations exceed loads, and the highest value is approximately 1450 kWh for 16:00 time slot as the loads exceed the generations. Using (5) and efficiency of 80%, the required storage capacity is approximately 3 MWh. Note that DA is rather idealistic, even though we have considered the variations in renewable generations.

Using NDA, computer simulations yield LOEE value of 5.32 MWh, and minimum storage capacity of 11 MWh. Thus, this approach is more conservative than DA. Daily renewable energy productions will be approximately 25 MWh, exceeding the college energy

consumptions of nearly 20 MWh. BEV battery storages will be utilized to smooth solar/wind intermittency, and shift power generation/load profiles. For BEV drivers in rural areas of New York State, probability distribution functions (PDFs) of arrival times and travel distance are obtained from National Household Travel Survey (NHTS) database [54]. To reflect BEV-Grid connection windows, we divide faculty, staff and students into two commuting groups, morning group with 200 BEVs and evening group with 75 BEVs. The first group includes teaching faculty, office staff and commuting students, who usually come to the campus in the morning, see Fig. II. B. 5(A). The second group includes research faculty, outreach staff and student-teachers who leave the campus after breakfast and come back around dinner time (Fig. II. B. 5(B)). The charging time for these groups may be delayed to properly manage the battery energy releases and storages, renewable energy productions and regular college energy loads [55]. The travel distance range for both groups is shown in Fig. II. B. 5(C). Please note that the horizontal axis beyond 160 km becomes non-linear to accommodate the statistical results for distances equal or larger than 170 km.



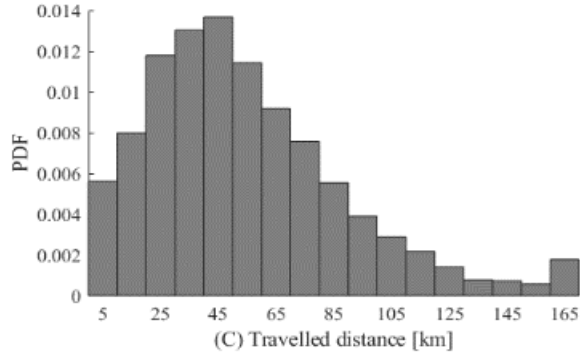


Figure II. B. 5. PDF of morning arrival time (A), evening arrival time (B) and travel distance (C)

In Table II. B. I, BEV vehicle types, market shares, drive-ranges and energies can be predicted by extrapolate data from NHTS and BEV manufacturers.

Table II. B. I. Assumed Characteristics of BEV

Vehicle Type	Expected Market Share (%)	Rated Power (kW)	Energy (kWh)	Single Charge Drive-Range (km)
Compact sedan	51.48	7.4	33	183
Mid-size sedan	10.35	11.5	75	417
Mid-size SUV	38.17	17.2	100	475

Generally, the travel distance range in Fig. II. B. 5(C) is less than the single-charge drive-range in Table II. B. I. College load is approximately 20 MWh and expected BEV loads is 5 MWh calculated using Monte Carlo simulation and the data from Fig. II. B. 5 and Table II. B. I. Additionally, spent BEV batteries will be utilized as a permanent energy storage system, with its storage capacity of 11 MWh calculated in previous section. According to the power generation/load needs, ESS will store the excess energy or release energy. When regional grids experience outages, an island may be formed to ensure balanced power between generations and consumptions.

#### D. Load Balance Equation

The load balance equation can be written as:

$$P_{College\ load}(t) + P_{ESS}(t) + P_{BEV}(t) = P_{Solar}(t) + P_{Wind}(t) + P_{Biomass}(t) \quad t = 1, 2, \dots, 24 \quad (12)$$

There will be three modes of operations:

1. If total renewable generation is less than the summation of  $P_{College\ load} + P_{BEV}$  then battery ESS needs to be discharged (i.e.  $P_{ESS} < 0$ )
2. If total renewable generation is more than the summation of  $P_{College\ load} + P_{BEV}$  and the uncertainty of the corresponding time slot is less than those of other time slots, battery ESS could be charged (i.e.  $P_{ESS} > 0$ ).
3. If total renewable generation is more than the summation of  $P_{College\ load} + P_{BEV}$  and the uncertainty of the corresponding time slot is more than those of other time slots, battery ESS will neither be charged nor discharged (i.e.  $P_{ESS} = 0$ ) and the extra renewable energy can be provided to outside via grid (as reserve to offset any unpredicted load increments).

To examine the load uncertainty imposed by random behaviors of BEV drivers, the confidence interval of mean for each time slot can be calculated by (13) [52].

$$\bar{X} - t_{\frac{\alpha}{2}}(n-1) \frac{s}{\sqrt{n}} \leq \mu \leq \bar{X} + t_{\frac{\alpha}{2}}(n-1) \frac{s}{\sqrt{n}} \quad (13)$$

where  $\bar{X}$  and  $s$  are the mean and standard deviation of a random sample of size  $n$  from the normal population,  $t_{\frac{\alpha}{2}}(n-1)$  is a  $t$ -distribution with  $n-1$  degrees of freedom, and  $\alpha$  is significance level. After simulating the BEV owners' driving habits, the random BEV load variable follows a normal distribution at each time slot.

Equation (13) is utilized to obtain uncertainty of random BEV load variable at each hour. Assuming that the confidence degree is equal to 95% ( $1 - \alpha = 95\%$ ), confidence interval of the mean at each hour for one day is calculated using (13), and plotted in Fig. II. B. 6. The battery ESS may be charged during time slots with small confidence interval values, such as 8:00 – 9:00, and 17:00 – 23:00. It has to be mentioned that confidence interval is reduced from 7:00 to 9:00 due to the demand response program (i.e. load shifting) to delay charging time for BEVs. For 10:00 – 14:00 and 2:00 – 6:00, large

variations occur because of on campus BEV charging and wind/solar energy intermittency receptively.

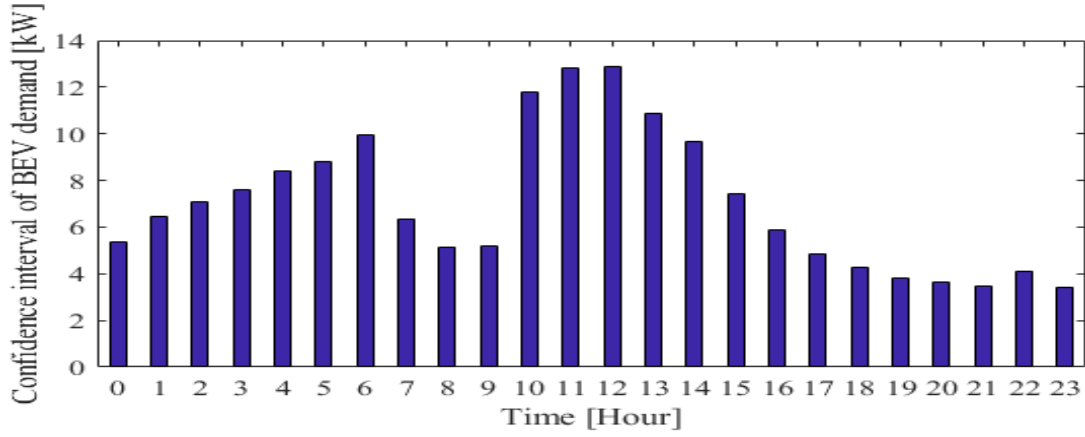


Figure II. B. 6. Confidence interval of mean for BEV load profile with sample of size 275 over 24 hours

### E. Simulation Results

Fig. II. B. 7 illustrates three hourly activities: 1. The left bar shows the renewable power generation and battery discharging; 2. The right bar shows the load power and battery charging; and 3. The number in the top circle shows the operation mode. Daily energy generations and consumptions are summarized in Table II. B. II, where energy balance can be achieved.

Table II. B. II. Energy Production and Consumption for Each Renewable Source and Demand for Expected Values of Random Variables

Type	Generation [MWh]	Consumption [MWh]
Wind	11.52	–
Solar	4.93	–
Biomass	8.97	–
College	–	19.14
Evening commuting BEV	–	1.34
Morning commuting BEV	–	3.57
Total	25.42	24.05

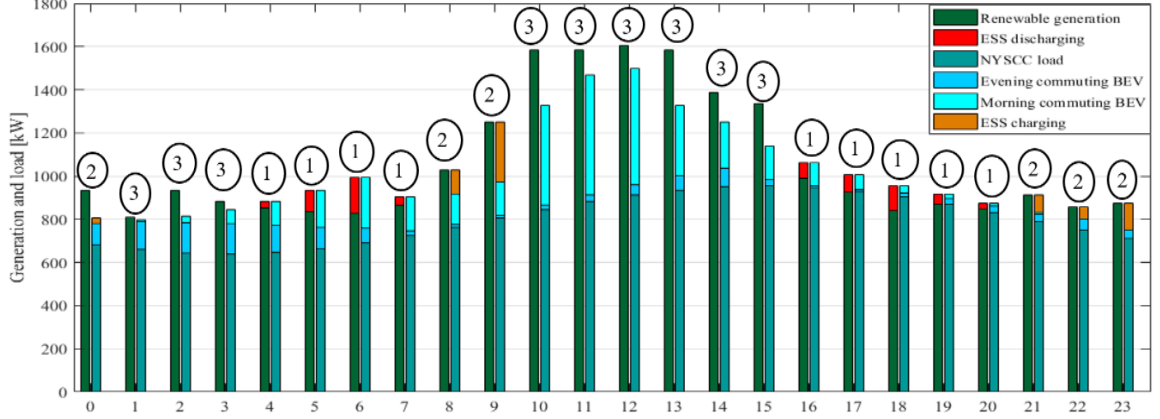


Figure II. B. 7. Hourly renewable power generation and battery discharging (left), load and battery charging(right), and operation mode for expected values of random variables

As it was already stated, in order to form an island on campus to meet the load (i.e. college and BEV load) 11MWh ESS has to be supplied from spent battery of electric vehicles. Also, using NDA, one can see that a total amount of 6.34 MWh is the extra amount of renewable generation available after 21:00 in Fig. II. B. 7 during a day. Considering the efficiency of the inverters (i.e. 80%) 5.072 MWh of this extra energy can be stored in ESS which is less than the calculated 11MWh capacity for ESS. In order to have 11MWh ESS capacity from spent battery of electric vehicles considering the market share percentage of different BEV models and the degrading effect of spent batteries (i.e. total capacity reduces by 85%) 205 spent batteries of electric vehicles is required to meet the load including college demand and commuting BEVs. Nevertheless, it is a practical assumption to say that BEVs are not allowed to work in charging mode during power outage (i.e. BEV demand is non-critical load). In this case we could either use spent batteries as ESS to meet the college load (i.e. critical load) or use the extra energy stored in BEVs (i.e. V2G operation mode) while there is no ESS available. For the latter solution (12) has to be modified as follows:

$$P_{College\ load}(t) = P_{Solar}(t) + P_{Wind}(t) + P_{Biomass}(t) + P_{BEV}(t) \quad t = 1, 2, \dots, 24 \quad (14)$$

The  $P_{BEV}$  on the right side of (14) indicates that the BEVs are acting as an energy source and sending power back to the grid.

It can be seen from the Fig. II. B. 7 that if the operator wants to plan based on the expected values, the renewable generation can always meet the college load. However,

there is no guarantee that renewables can always produce their expected values due to their intermittent nature. There are many scenarios that the college load is more than that of generation. As a result, the state sampling method has to be used to appropriately determine the number of BEVs working in V2G mode or the required ESS capacity from spent batteries in order to meet the college load when there is lack of production from renewables.

Using the calculation explained in this section, the minimum storage capacity to meet the college load would be 5.32 MWh. Eighty five BEVs or 100 spent batteries will be required to provide this amount of energy. It is noteworthy that by assuming the minimum SOC of 40% in V2G operation mode, the BEV owners can be sure that they have got enough energy to drive back home.

In the second scenario we assume that the rated power generation for wind and solar are doubled by installing additional 2 megawatt wind turbine and 2 megawatt solar panels. In this case, the required storage capacity reduces to 3.74 MWh. Therefore, the number of required BEVs working in V2G during islanded operation goes down by 25. Also, the number of spent batteries decreases by 30 and becomes 70.

In the first sight, it seems that by expanding renewable energy generation production, the number of required BEVs both in terms of V2G and spent battery goes down. One should notice that during the normal operation of the grid (i.e. grid connected) a huge amount of wind and solar generation should be provided to the outside via grid if there is no ESS. For the second scenario the total available extra renewable generation for one day is equal to 16 MWh which is much higher than the required ESS capacity determined in both V2G and spent battery scenarios. For instance, 255 BEVs is needed to store this much of energy which is more than that of other scenarios. For several different scenarios, representative numbers and capacities of batteries are summarized in Table II.

B. III.

Table II. B. III. Summary of Number of BEVs and ESS For Normal and Power Outage Condition

Scenario	Grid connected		Islanding		
	Total extra renewable [MWh]	No. of BEVs for extra energy	Required ESS capacity [MWh]	No. of BEVs (V2G)	No. of spent batteries (Idle)
2MW wind & 2MW solar	5.07	81	5.32	85	100
4 MW wind & 4MW solar	16	255	3.74	60	70

From the table above, one can realize that resilience improvement during power outage and extra energy saving during normal operation may be two chief reasons for policy makers and system operators to raise incentives for BEV purchases. For future planning horizon if the renewable sources keep increasing, the number of BEVs has to go up inevitably in order to store the extra energy and confront the intermittency of renewables.

For electricity rates between \$0.10 and \$0.20 per kWh, the daily (annual) budget for 25 MWh would be \$2.5K-\$5K (\$912.5K-\$1,825K) [56]. In 2015, the average construction cost for new power plant was \$1 - \$3 per watt, with solar PV being \$2.921 per watt [57]. In the last two years, the cost of solar PV generation construction was reduced to \$1 per watt [58]. General site maintenance cost is \$0.2 - \$3 per kilowatt per year [59]. For wind, similar trend in cost reduction is observed [60]. Recently, EIA published its cost predictions for 2019, 2022 and 2040, respectively [61]. If cost reductions can be realized, one can justify future additions for renewable energy in electricity productions. BEV costs are usually in three folds: 1. Batteries, 2. Vehicles and 3. Ownerships. In 2016, the battery cost was nearly \$227 per kW-Hr, and the average vehicle cost was approximately \$50K [62], [63]. For a BEV with 50 kWh battery, the cost of the battery would be \$11,350 which is a significant portion of the overall vehicle cost. As predicted by US Department of Energy, the targeted battery cost will be reduced to \$125/kWh in several years [64]. Using a consumer centric model, Total Ownership Costs (TOC) for BEV should be cheaper than that of PHEV or internal combustion engine vehicle (ICEV) [65]. From the technical point of view, more electricity from renewables would lead higher BEV demands. From

economic point of views, one needs to systematically and empirically examine the relationships between the demands and renewables, along with other socioeconomic factors.

### **III. CONCLUSION AND DISCUSSIONS**

Based on technical principles and empirical examinations, renewables impact BEV demands positively. Holding other variables constants, one percent increment in renewables would yield 2% increment in BEV demands per 100 thousand people. Since BEV may potentially benefit both environment and energy sectors, governments should promote renewables and battery storages, which can compensate solar/wind intermittency and adjust power grid peak/valley fluctuations. High gasoline prices would lead to high BEV demands. In terms of BEV demand density, Norway, France and Sweden ranked first three places in 2016; which took first, fifth and third places for gasoline prices, respectively. Presumably, gasoline prices can be utilized as a policy tool to stimulate BEV demands. The number of chargers impacts BEV demands positively. Business/urban/community planners should properly select locations that are close to public parking facilities, highway rest areas, shopping centers and community activity centers. Utilities should incorporate power grids (smart grids and micro-grids), renewables and charging stations to provide convenience to BEV users. For example, near the college in Western New York, there are several suitable locations: 1. College town with solar/wind/biomass sources, parking lots and substations; 2. Wood processing facilities, cheese factories, and/or dairy farms near major highways; 3. Major shopping centers with factories nearby; and 4. County government buildings. Population density does impact BEV demands positively. BEV marketing/sales should be mainly targeting the large population centers. Since education levels impact BEV demands slightly, one may select such centers with high education levels. The elasticity for GDP per capita is larger than one. If manufacturers can reduce BEV prices, the demands will increase substantially. Governments may provide tax incentives to BEV consumers.

## C. Cloud Computing Based Real-Time Energy Management System with RNN-LSTM Wind Forecasting

### I. INTRODUCTION

By 2030, the renewable energy penetration level in New York State's electric power generation will be 50%. New wind farms are being proposed, planned and installed in upstate New York.

The downstate region of New York (Long Island, New York City, and the Hudson Valley) annually uses 66% of the state's electric energy. Yet, that region's power plants generate only 53% of the state's electricity<sup>1</sup>. Enabling upstate resources to better serve downstate consumers [66].

Local consumptions with energy storages such as batteries can be formed in distribution network; one can envision a resilient power network to resist power outages due to extreme weather and other unexpected events. Forming a community power island may be beneficial to use the upstate wind power resources

We propose a method to combine Energy Storage Systems (ESS), loads, and renewable sources which can operate as a microgrid during main grid outages.

With Internet of Things (IoT) and Real-Time Hardware-in-Loop (RT-HIL), one can monitor and control power flows.

Machine learning and cloud computing can be utilized for 10 minutes ahead renewable generation prediction. Recurrent Neural Networks (RNN) with Long Short-Term Memory (LSTM) method is used for wind power production.

### II. METHODOLOGY

#### A. OPAL-RT HIL Simulation

A microgrid testbed is used for simulation which could be considered as a representation of Alfred power grid.

Wind power generation data from a system of 100 kW wind turbine located on Alfred State College campus are used.

### B. RNN-LSTM for Wind Forecasting

RNN allows to connect previous information to the present state such as wind power forecasting.

In some cases, where the gap between the relevant information and the place that it's needed to be predicted is small, RNNs can learn to use the past information (Fig. II. C. 1). However, as that gap grows, RNNs become unable to learn to connect the information. LSTMs are a special kind of RNN, capable of learning long-term dependencies (Fig. II. C. 2) [66].

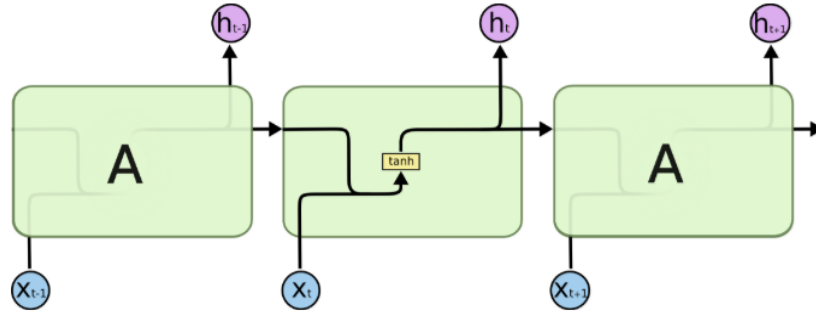


Figure II. C. 1. Standard RNN

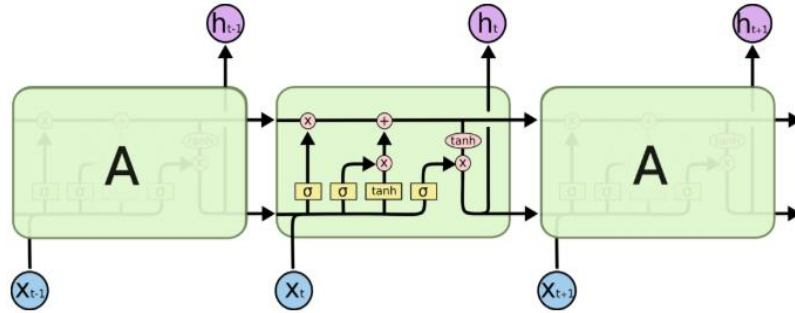


Figure II. C. 2. RNN-LSTM

### C. Experimental Design

The LSTM structure is depicted in Fig. II. C. 3, where  $X_t$  is the real time wind power generation acquired from IoT data acquisition system,  $h_t$  is the hidden state which can be represented by the previous state  $h_{t-1}$  and the current input  $X_t$  under a control of a set of weight coefficient (stored as the short-term memory), and  $C_t$  is the cell state which keeps long short-term memory (seasonal or monthly information of historical data) and  $C_{t-1}$  will be trained along with  $h_{t-1}$  to the updated  $C_t$ .

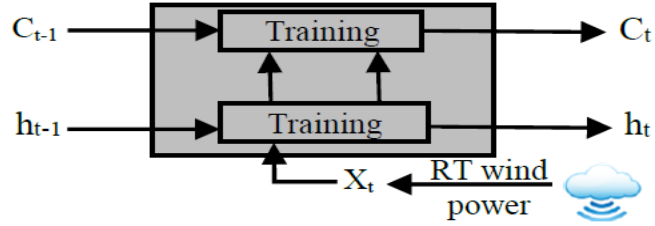


Figure II. C. 3. LSTM structure for wind power forecasting

The predicted output is sent to simulated renewable energy integrated power system (OPAL-RT), and real time response of the entire system is monitored to ensure system security constraint compliances by generating correction control signals as shown in Fig. II. C. 4.

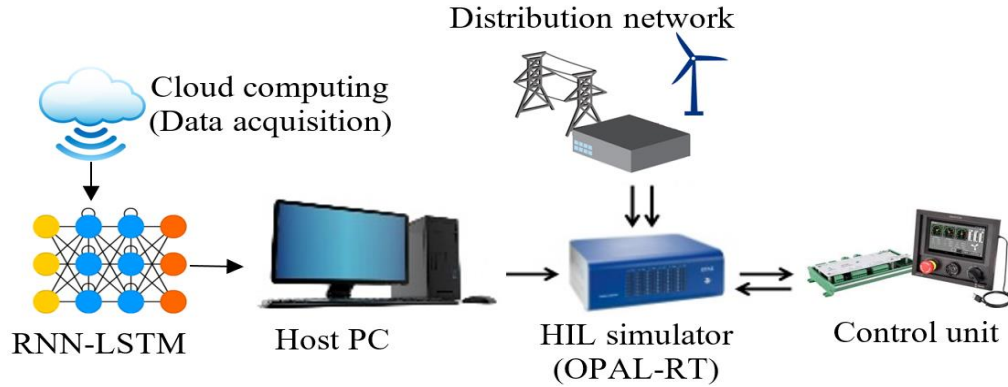


Figure II. C. 4. Real-time testbed for microgrid studies along with IoT infrastructure for wind forecasting.

### III. SIMULATION RESULTS

#### A. Wind Forecasting Results

Fig. II. C. 5 shows the output results of using RNN-LSTM for wind power forecasting. After initial “machine learning,” the predication yields close resemblance of actual data. It takes 20 seconds to forecast the next 10 minutes’ wind speed, indicating a promising methodology for real-time operation.

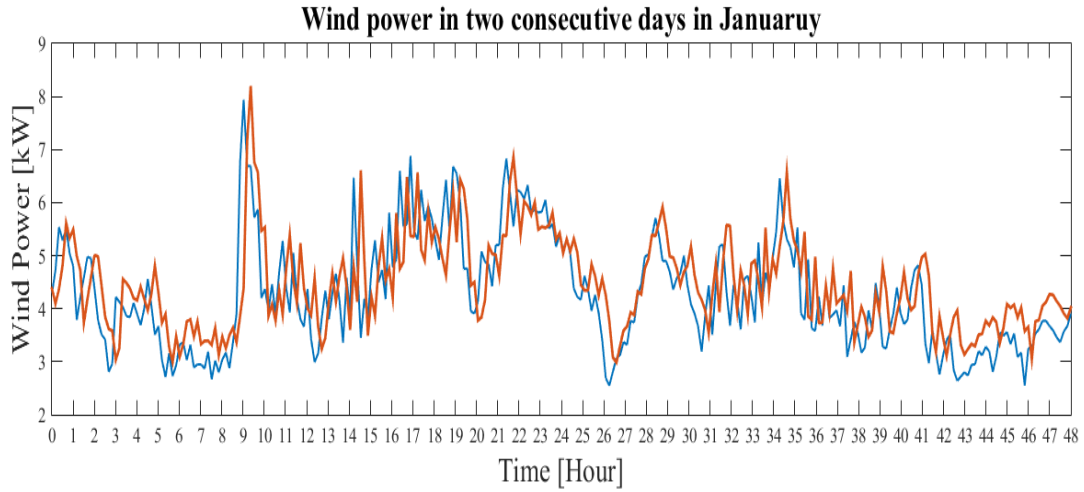


Figure II. C. 5. Wind power prediction along with actual wind power production

### *B. Microgrid Testbed*

The microgrid model which is implemented in OPAL-RT is shown in Fig. II. C. 6 and generation/load capacities are summarized in Table II. C. I [68].

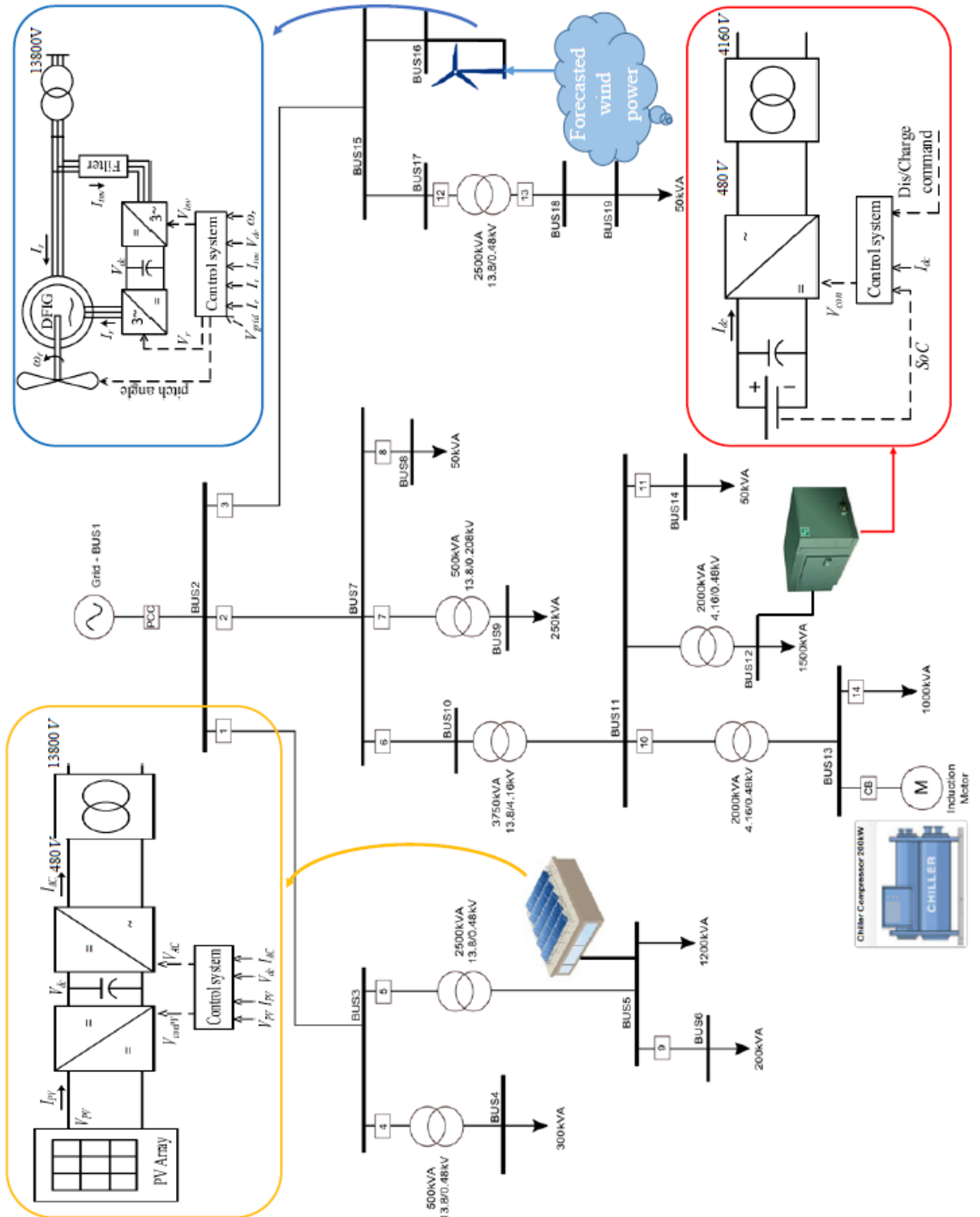


Figure II. C. 6. Microgrid testbed

Table II. C. I. Generation/Load Data

<b>Generation or Storage Capacity</b>	
Wind turbine rated power	1.5MW
PV system rated power	1.5 MW
Energy Storage System capacity	300 kWh (625 Ah, 480 V)
<b>Load</b>	
System total static load	4.07 MW
Motor rated power	200kW

*C. Real-Time Simulation*

Two scenarios are considered for real-time simulation of the microgrid presented in the previous section along with the wind power production forecasting.

In the first scenario predicted wind power is imported to the system and the behavior of the system is studied. Extra wind power generation can be stored in the energy storage system and when the storage is fully charged, the extra power goes back to the grid as shown in Fig. II. C. 7.

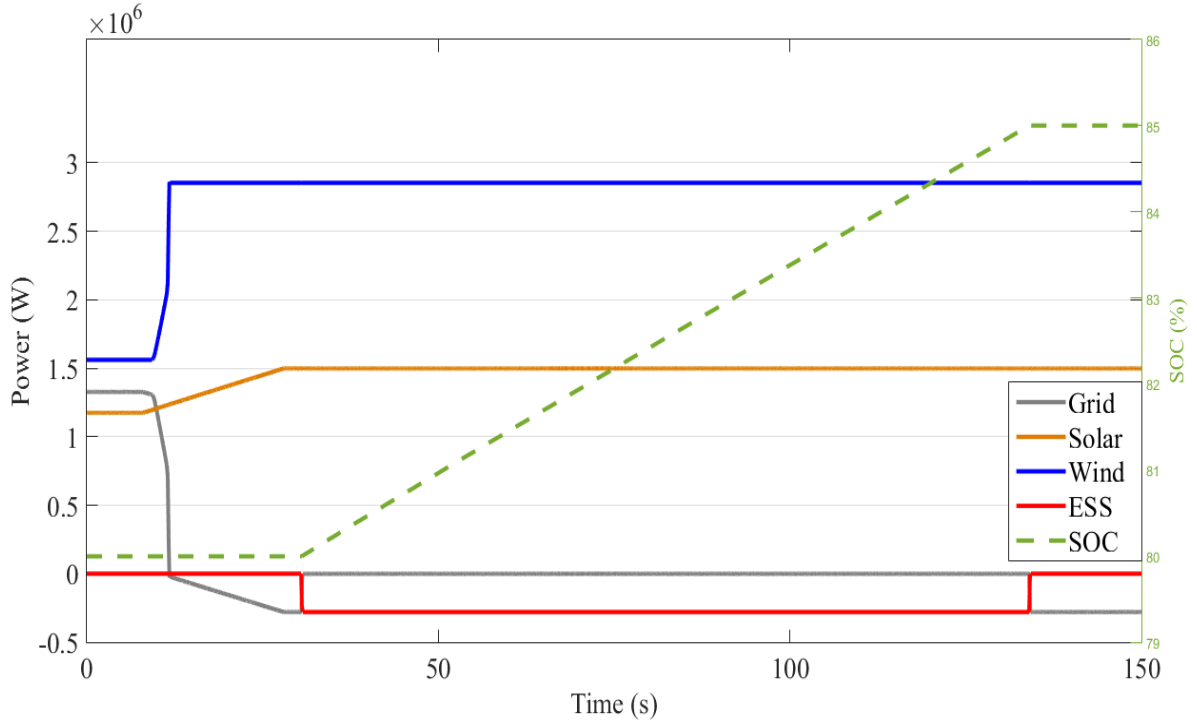


Figure II. C. 7. Active power generation of different units.

The state charge of the battery along with renewable generation is summarized in Table II. C. II for before and after of wind power variation.

Table II. C. II. Generation of Different Components For Different Wind Speeds

Current State	
SOC	80 %
Grid	1.33 MW
Wind	1.57 MW
Solar	1.17 MW

Next Forecasting Time Interval	
SOC	85 %
Grid	0
Wind	2.9 MW
Solar	1.5 MW
ESS	-300 kW (Charging)

In the second scenario it is assumed that a fault occurs on the main grid and the microgrid is disconnected from the main grid (i.e. islanding operation mode). During the fault condition, the induction motor is switched off because it is assumed that it is a non-critical load. After a few seconds the fault is cleared from the main grid and the microgrid gets connected to the main grid (i.e. normal operation mode). The transient response of the motor is represented in Fig. II. C. 8. Values of Microgrid variables are shown in Table II. C. III.

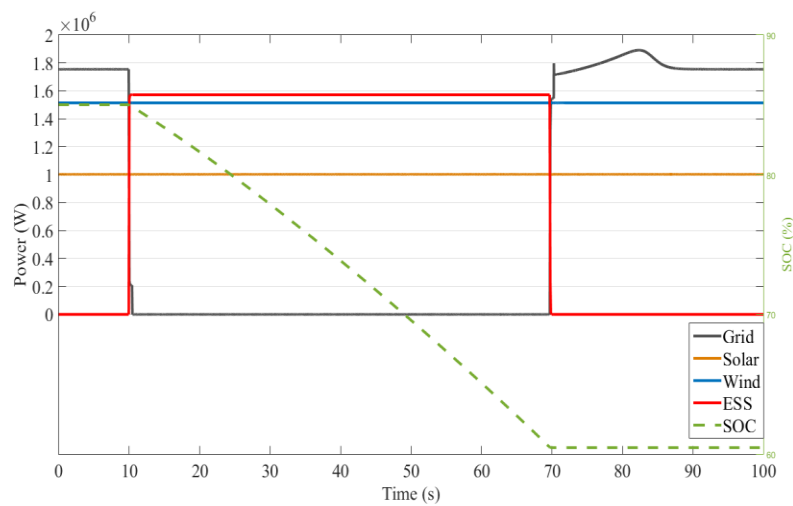


Figure II. C. 8. Active power generation before and after of fault occurrence

Table II. C. III. Different Component Generation Status for Different Operation Mode

<b>Current State</b>	
SOC	85 %
Grid	1.75 MW
Wind	1.5 MW
Solar	1MW
Motor	200 kW
<b>Islanding</b>	
Grid	0
Motor	0
ESS	1.6 MW (Discharging)
<b>Post Fault</b>	
SOC	60 %
Grid	1.75 MW
Motor	200 kW
ESS	0

#### **IV. CONCLUSION AND FUTURE WORK**

In wind power prediction a latency can be seen in the forecasted wind power. Such time delay can be corrected by systematically shifting the time. In first scenario the inverter rating should be able to handle 300kW and in the second scenario the inverter rating should at least handle 1.6 MW which means that several inverter units need to be used in parallel.

The future work of this study could be designing a real-time energy management system with live data from wind turbines nearby, harvested via IoT data acquisitions systems and also implementing a control system to use the ESS in order to compensate for the wind power forecast error.

### III. UNPUBLISHED WORK

New York Independent System Operator (NYISO) as an independent entity is responsible for operating and monitoring New York State bulk power system. Data required by the NYISO to carry out technical analysis to support its mission of preserving the reliability of the New York State bulk electric systems are used to model and simulate power grids.

Actual and forecast data of all the components, including loads, are required to analyze, study, and plan the interconnected electric systems. Detailed data of system components must be maintained and updated by the facility owners and load-serving entities and provided to the NYISO accurately. Complete, accurate, and timely data are needed by the NYISO to prepare system analyses to assess reliability of the New York State bulk electric systems. System analyses include steady-state, short circuit, and dynamic simulations of the electrical networks. Data requirements for these system analyses include information on system components, system configurations, facility ratings, customer demands, and electric power transactions. This manual describes specific data supplied by the New York Control Area (NYCA) facility owners and collected by the NYISO for these purposes [71].

Upon receiving and then validating the data, the system modeling group in NYISO uses these data to simulate power grid models in a commercial software package called “PSS/E” which is a powerful tool developed by Siemens for power system studies. PSS/E can handle a model containing thousands of buses and the system modeling group uses it for steady state analysis.

The system modeling group has to work with large data sets. A programming tool is required to handle these large data. For example, Python is an increasingly popular tool for data analysis, which can be used for manipulating, processing, cleaning, and crunching data.

In PSS/E, each analysis has to be carried out through the Graphical User Interphase (GUI) manually. In order to automate the processes of data screening and checking, an interface module is developed by PSS/E in order to create a connection between PSSE and python. This feature will grant the user to have complete access over the power system

parameters. By utilizing the PSS/E-Python interface module, the user would be able to alter the existing network parameters, run different studies such as power flow and contingency analysis and eventually generate excel file reports.

In the following subsections, the process of building a power system model in PSS/E is first explained and then a python code is presented to show the applications of PSS/E-Python interface modules.

### A. PSS/E model

Each power system model is composed of basic elements including transmission lines, generators, loads, transformers and buses. In PSS/E, a separate tab is assigned for each of these components. There are other tabs for advanced studies if required. Five (5) bus Siemens sample case is used here as an example for implementing python code. In Fig. III. 1. different tabs are shown. The five (5) bus case data should be entered accordingly in each tab.

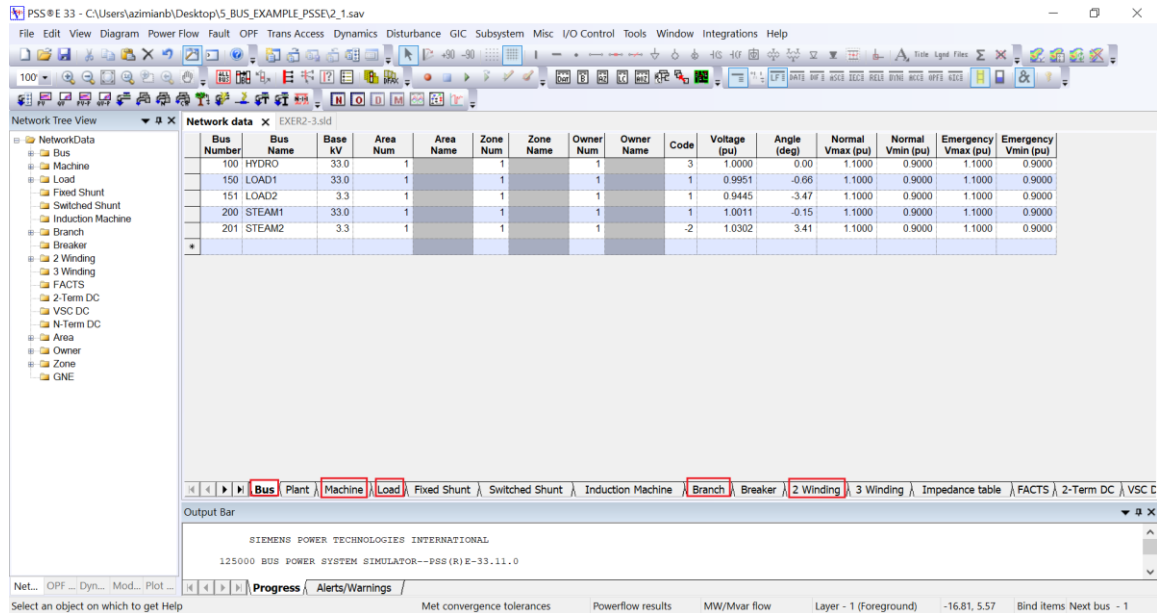


Figure III. 1. PSS/E GUI environment for input data

After building the power system model, power flow should be run to determine transmission line flows and voltage magnitudes. Power flow solution can be found under power flow menu as shown in Fig. III. 2.

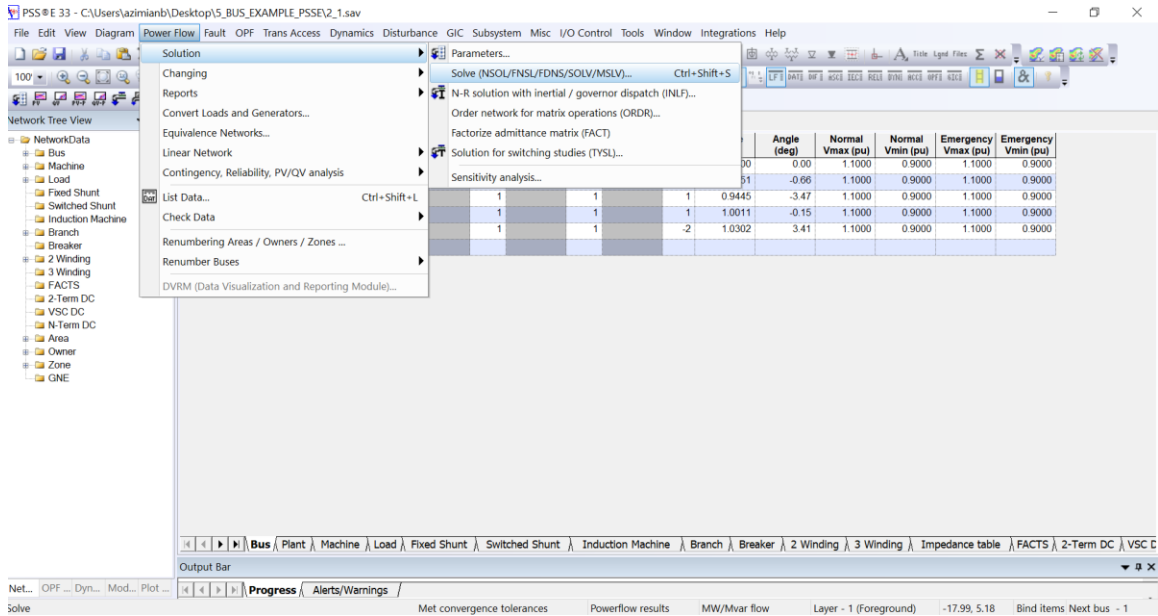


Figure III. 2. Running power flow analysis from PSS/E GUI

After running power flow, network diagram can also be drawn in order to see the line active and reactive flows and corresponding direction as well as generation dispatches. The percentage on each line above the colored rectangle is showing the loading percentage. For each line, three rates are defined. Rate A which refers to normal ratings. Rate B refers to long term emergency ratings and rate C refers to short-term emergency ratings. Considering these three ratings, corrective measures have to be considered if the limits are passed.

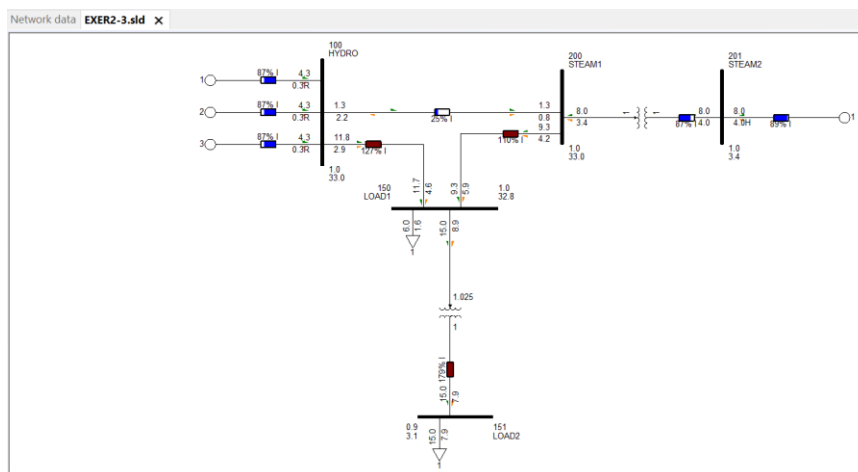


Figure III. 3. 5 Bus system diagram with line flows

## B. PSSE/Python Interface

As it was seen in the previous section, there could be a number of limit violations in power systems. For example, a generating unit must be flagged if it is generating more than its maximum active generation capacity. Also, the generation unit has to be identified if its reactive generation is more/less than its upper/lower reactive limit. This violation identification has been implemented in python script which is represented below. In python programming language ‘#’ is used for writing comments. At the top of each block of code, a ‘#’ symbol is followed by a brief explanation for better understanding.

```
##### making connection between PSSE and Python
import os
import sys
PSSE_PATH = r'C:\Program Files (x86)\PTI\PSSE33\PSSBIN'
sys.path.append(PSSE_PATH)
os.environ['PATH'] += ';' +PSSE_PATH
#-----

##### importing PSSE module
import psspy
psspy.throwPsseExceptions = True           # closing pop up windows
import redirect                             # closing pop up windows
redirect.psse2py()                          # closing pop up windows
#-----

##### importing pandas for excel representation
import pandas as pd

#-----

##### running the case system (VERY IMPORTANT NOTE: if
you already run the case and have the power flow results in SAV
file comment the next section)
```

```

psspy.psseinit(107000)
psspy.case(r'C:\Users\azimianb\Desktop\5_BUS_EXAMPLE_PSSE\2_1.sav
')
#-----
    ### running power flow and changing data (comment this
section if your SAV file already has the power flow results)
ierr = psspy.load_chng_4(150, '1', realar1 = 6, realar2 = -10) #
original values 6 and 1.6
ierr = psspy.fdns()
#-----
    ### initializing the default values (for more info see
pages 2213 to 2215 of API)
cdef = psspy.getdefaultchar()
idef = psspy.getdefaultint()
rdef = psspy.getdefaultreal()
#-----
    ### Checking active and reactive power generation
limits for each generator
machineVios_P = [[],[],[ ]]
noMachineVios_P = True
machineVios_Q = [[],[],[ ]]
noMachineVios_Q = True
ierr, busses = psspy.abusint(-1, 1, ['NUMBER', 'TYPE'])
for i in range(len(busses[0])):
    bus = busses[0][i]
    if busses[1][i] == 2 or busses[1][i] == 3:
        err1 = psspy.inimac(bus)
        while err1 == 0:      #If err1 = 1, no more machines @ bus
            err1,wid = psspy.nxtmac(bus)
            err2,unit_pmin = psspy.macdat(bus,wid,'PMIN')
            err3,unit_pmax = psspy.macdat(bus,wid,'PMAX')

```

```

err4,unit_pgen = psspy.macdat(bus,wid,'P')
err5,unit_qmin = psspy.macdat(bus,wid,'QMIN')
err6,unit_qmax = psspy.macdat(bus,wid,'QMAX')
err7,unit_qgen = psspy.macdat(bus,wid,'Q')
if unit_pmax < unit_pgen:
    noMachineVios_P = False
    machineVios_P[0].append(bus)
    machineVios_P[1].append(wid)
    machineVios_P[2].append(unit_pgen-unit_pmax)
if unit_pmin > unit_pgen:
    noMachineVios_P = False
    machineVios_P[0].append(bus)
    machineVios_P[1].append(wid)
    machineVios_P[2].append(unit_pgen-unit_pmin)
if unit_qmax < unit_qgen:
    noMachineVios_Q = False
    machineVios_Q[0].append(bus)
    machineVios_Q[1].append(wid)
    machineVios_Q[2].append(unit_qgen-unit_qmax)
if unit_qmin > unit_qgen:
    noMachineVios_Q = False
    machineVios_Q[0].append(bus)
    machineVios_Q[1].append(wid)
    machineVios_Q[2].append(unit_qgen-unit_qmax)

#-----

    ### creating excel results
from win32com.client import Dispatch
excel = Dispatch("Excel.Application")
workbook = excel.Workbooks.Open(r'C:\Users\azimianb\Desktop\5_BUS_EXAMPLE_PS
SE\Results')

```

```

map(lambda book: book.Close(False), excel.Workbooks)
excel.Quit()

P_data = pd.DataFrame({'Bus number':machineVios_P[0][:],'Generator
ID':machineVios_P[1][:],'Delta_P,+: upper limit passed, -: lower
limit passed':machineVios_P[2][:]})
Q_data = pd.DataFrame({'Bus number':machineVios_Q[0][:],'Generator
ID':machineVios_Q[1][:],'Delta_Q,+: upper limit passed, -: lower
limit passed':machineVios_Q[2][:]})
writer = pd.ExcelWriter("Results.xlsx",engine = 'xlsxwriter')
P_data.to_excel(writer, sheet_name='P', startrow=1, header=False)
Q_data.to_excel(writer, sheet_name='Q', startrow=1, header=False)
# Get the xlsxwriter workbook and worksheet objects.
workbook = writer.book
# Add a header format for excel file report
header_format = workbook.add_format({
    'bold': True,
    'text_wrap': True,
    'valign': 'top',
    'align': 'center',
    'fg_color': '#D7E4BC',
    'border': 1})
# Write the column headers with the defined format.
data_list = [P_data, Q_data]
data_list1 = ['P', 'Q']
# Adjusting column headers length
for i,j in zip(data_list,data_list1):
    worksheet = writer.sheets[j]
    if len(i)!= 0:      # for the case when there is no violation
otherwise it causes a kernel restating problem
        for col_num, value in enumerate(i.columns.values):

```

```

        worksheet.write(0, col_num + 1, value, header_format)
for k, col in enumerate(i.columns):
# find length of column i
        column_len = i[col].astype(str).str.len().max()
# Setting the length if the column header is larger
# than the max column value length
        column_len = max(column_len, len(col)) + 2
# set the column length
        worksheet.set_column(k+1, k+1,
column_len,header_format)
    else:
        c = 2
        i = pd.DataFrame({'no violation': ['No '+j+' violation']})
        i.to_excel(writer, sheet_name=j, startrow=1, header=False)
writer.save()
file =
r'C:\Users\azimianb\Desktop\5_BUS_EXAMPLE_PSSE\Results.xlsx'
os.startfile(file)

```

For the five (5) bus case, the power output of each generator is between its maximum ( $P_{\max}$ ) and minimum ( $P_{\min}$ ) capacity. In order to see the applicability of the code, the load at bus 150 is scaled up. After running power flow, it can be seen that generators at swing bus have to go above their limits to meet the loads. This will result in limit violation which is reported in excel format as shown below.

	Bus number	Delta_P,+ : upper limit passed, - : lower limit passed	Generator ID
0	100	4.019778252	1
1	100	4.019778252	2
2	100	4.019778252	3
	Bus number	Delta_Q,+ : upper limit passed, - : lower limit passed	Generator ID
0	100	-5.477796555	1
1	100	-5.477796555	2
2	100	-5.477796555	3

Figure III. 4. Snapshot of excel file output for violation report

The results above indicate that each of the three generators at bus 100 have to go above their active limit by about 4 MW and go below their reactive limit by 5.4 MVAR. The results are verified directly by PSS/E GUI report shown in Fig. III. 5.

Bus Number	Bus Name	Id	Area Num	Area Name	Zone Num	Zone Name	Cod e	VSched (pu)	Remote Bus Number	In Service	PGen (MW)	PMax (MW)	PMin (MW)	QGen (Mvar)	QMax (Mvar)	QMin (Mvar)	Mbase (MVA)	R
100	HYDRO 33.000	1	1		1		3	1.0000	0	<input checked="" type="checkbox"/>	9.0250	5.0000	0.0000	-3.4786	2.0000	0.0000	5.00	
100	HYDRO 33.000	2	1		1		3	1.0000	0	<input checked="" type="checkbox"/>	9.0250	5.0000	0.0000	-3.4786	2.0000	0.0000	5.00	
100	HYDRO 33.000	3	1		1		3	1.0000	0	<input checked="" type="checkbox"/>	9.0250	5.0000	0.0000	-3.4786	2.0000	0.0000	5.00	
201	STEAM2 3.3000	1	1		1		-2	1.0500	200	<input checked="" type="checkbox"/>	8.0000	10.0000	0.0000	4.0000	4.0000	0.0000	10.00	

Figure III. 5. PSS/E power flow results for scaled up load at bus 150

### C. Conclusion

To have a reliable electric grid, power systems have to be modeled accurately to ensure reliability. Data collection is the first step on this path. The system modeling group in NYISO is responsible for collecting data from Transmission Owners (TOs) and Generator Owners (GOs). After the data is pre-screened, they are imported to PSS/E software for different studies. To automate the screening and checking process, the PSS/E-python module needs to be used.

It is highly recommended to teach both PSS/E and Python to students in renewable energy program at Alfred University as these two softwares are widely used by NYISO and it could be a piece of valuable knowledge for their future career life.

## IV. SUMMARY AND CONCLUSIONS

This study focuses on the investigation of microgrids with energy storages. Two types of energy storage approaches were presented. First the BEVs can be used in V2G mode to send power back to the grid during fault condition or peak demand. Second, the spent batteries from BEVs can be used as ESS to store the extra energy of renewables during high wind and solar radiation.

The impact of renewable penetration and energy storage systems was studied in two time horizons. First day ahead approach was considered and planning and energy management practices were presented considering the uncertainty of renewables and BEV owners' driving behavior.

It was seen that, by implementing demand response program which runs based on stackelberg theory it is possible to reduce energy generation cost by almost 20%. In addition, the V2G feature of BEVs could help the grid operator to smooth the daily load profile. Reduced demand, during peak hours will have many advantageous such as alleviating the need for new conventional power plants [69].

Regarding the required number of BEVs or spent batteries, the grid operator could expect to utilize the capacity of 85 BEVs or 100 spent batteries in order to form an island with a microgrid which accommodates 2 MW wind, 2 MW solar and 400 kW biomass generation. By doubling the wind and solar capacity (i.e. 4 MW each) the required number of BEVs and spent batteries decreases by 30 and 25 respectively.

After the day ahead approach, the real-time operation of the microgrid was simulated in OPAL-RT. Dynamic response of different components such as ESS and induction motor was presented before, during, and post fault condition.

In the process of day ahead planning of BEVs and renewable energies in microgrid it was seen that there is a correlation between renewable energy and BEVs expansion planning.

For the studied microgrid, if renewable energy capacity is expanded by twofold, the purchase demand for BEVs will increase by threefold. Consequently, more BEVs could help the grid operators to increase the flexibility and resiliency of the power system.

## V. FUTURE WORK

In the application of Stackelberg game theory for demand response program renewable energy units was not included. The next step in order to improve the model could be adding random models of wind and solar in the game theory structure [70].

In day ahead planning and energy management of microgrids with BEVs section, minimum number of BEVs and spent batteries were found separately to confront the uncertainties imposed by renewables. Cost/benefit optimization analysis can be carried out to find the optimum number of BEVs and spent batteries together.

In the area of real time simulation average model of inverter was used for renewables units in MATLAB/Simulink. It is suggested to implement detailed model of inverter in OPAL-RT. However, high frequency switching puts a huge computing load on the processor which may cause some problems for real time operation.

## VI. REFERENCES

1. Mondal A, Misra S, Patel LS, Pal SK, Obaidat MS. DEMANDS: Distributed Energy Management Using Noncooperative Scheduling in Smart Grid. *IEEE Syst J*. 2017;12(3):2645-53.
2. Gungor VC, Sahin D, Kocak T, Ergut S, Buccella C, Cecati C, Hancke GP. A survey on smart grid potential applications and communication requirements. *IEEE Trans Ind Informatics*. 2012;9(1):28-42.
3. Yu M, Hong SH. Supply–demand balancing for power management in smart grid: A Stackelberg game approach. *Appl Energ*. 2016;164:702-10.
4. Jia L, Tong L. Dynamic pricing and distributed energy management for demand response. *IEEE Trans Smart Grid*. 2016;7(2):1128-36.
5. Medina J, Muller N, Roytelman I. Demand response and distribution grid operations: Opportunities and challenges. *IEEE Trans Smart Grid*. 2010;1(2):193-8.
6. Metke AR, Ekl RL. Security technology for smart grid networks. *IEEE Trans Smart Grid*. 2010;1(1):99-107.
7. Moslehi K, Kumar R. A reliability perspective of the smart grid. *IEEE Trans Smart Grid*. 2010;1(1):57-64.
8. Parvania M, Fotuhi-Firuzabad M, Shahidehpour M. Optimal demand response aggregation in wholesale electricity markets. *IEEE trans Smart Grid*. 2013;4(4):1957-65.
9. Ahmadian S, Vahidi B, Jahanipour J, Hoseinian SH, Rastegar H. Price restricted optimal bidding model using derated sensitivity factors by considering risk concept. *IET Generation, Transmission & Distribution*. 2016;10(2):310-24.
10. Wei W, Liu F, Mei S. Energy pricing and dispatch for smart grid retailers under demand response and market price uncertainty. *IEEE Trans Smart Grid*. 2014;6(3):1364-74.
11. Chen J, Yang B, Guan X. Optimal demand response scheduling with Stackelberg game approach under load uncertainty for smart grid. Paper presented at: 2012 IEEE third international conference on smart grid communications (SmartGridComm); 2012 Nov 5; Tainan, Taiwan. (pp. 546-551). New York: IEEE, 2012.
12. Chen J, Zhu Q. A Stackelberg game approach for two-level distributed energy management in smart grids. *IEEE Trans Smart Grid*. 2017;9(6):6554-65.
13. Liu N, Yu X, Wang C, Wang J. Energy sharing management for microgrids with PV prosumers: A Stackelberg game approach. *IEEE Trans Ind Informatics*. 2017;13(3):1088-98.
14. El Rahi G, Etesami SR, Saad W, Mandayam NB, Poor HV. Managing price uncertainty in prosumer-centric energy trading: A prospect-theoretic Stackelberg game approach. *IEEE Trans Smart Grid*. 2017;10(1):702-13.

15. Belgana A, Rimal BP, Maier M. Open energy market strategies in microgrids: A Stackelberg game approach based on a hybrid multiobjective evolutionary algorithm. *IEEE Trans Smart Grid*. 2014;6(3):1243-52.
16. Azad S, Ghotbi E. A game equilibrium model of a retail electricity market with high penetration of small and mid-size renewable suppliers. *Elec J*. 2017;30(5):22-9.
17. Zhou Y, Gao F, Ci S, Yang Y, Xu Y. Time-of-use pricing in retail electricity market: Step tariff vs. usage-based schemes. Paper presented at: 2016 International Conference on Probabilistic Methods Applied to Power Systems (PMAPS); 2016 Oct 16; Beijing, China. (pp. 1-5). New York: IEEE, 2016.
18. Zhao T, Li Y, Pan X, Wang P, Zhang J. Real-time optimal energy and reserve management of electric vehicle fast charging station: Hierarchical game approach. *IEEE Trans Smart Grid*. 2017;9(5):5357-70.
19. Mediawathe CP, Smith DB. Game-Theoretic Electric Vehicle Charging Management Resilient to Non-Ideal User Behavior. *IEEE Trans Intel Transport Syst*. 2018;19(11):3486-95.
20. Gao B, Zhang W, Tang Y, Hu M, Zhu M, Zhan H. Game-theoretic energy management for residential users with dischargeable plug-in electric vehicles. *Energies*. 2014;7(11):7499-518.
21. Zhu Z, Lambbotharan S, Chin WH, Fan Z. A mean field game theoretic approach to electric vehicles charging. *IEEE Access*. 2016;4:3501-10.
22. Sarker A, Li Z, Kolodzey W, Shen H. Opportunistic energy sharing between power grid and electric vehicles: A game theory-based pricing policy. Paper presented at: 2017 IEEE 37th International Conference on Distributed Computing Systems (ICDCS); 2017 Jun 5-8; Atlanta, Georgia. (pp. 1197-1207). New York: IEEE, 2017.
23. Li B, Kisacikoglu MC, Liu C, Singh N, Erol-Kantarci M. Big data analytics for electric vehicle integration in green smart cities. *IEEE Commun. Mag*. 2017;55(11):19-25.
24. Ahmadian A, Sedghi M, Aliakbar-Golkar M, Fowler M, Elkamel A. Two-layer optimization methodology for wind distributed generation planning considering plug-in electric vehicles uncertainty: A flexible active-reactive power approach. *Energ Convers Manag*. 2016;124:231-46.
25. Tesla, Charging upon arrival. Accessed on: 2019 Aug 10. Available at: <https://www.tesla.com/destination-charging>
26. BMW, I3 customer manual overview, 2019 BMW of North America. Accessed on: 2019 Aug 10. Available at: <https://www.bmwusa.com/vehicles/bmwi/bmw-i3.html>
27. United States Energy Information Administration, "International Energy Outlook," 2017. Accessed on: 2019 Aug 10. Available at: [https://www.eia.gov/outlooks/ieo/pdf/0484\(2017\).pdf](https://www.eia.gov/outlooks/ieo/pdf/0484(2017).pdf)
28. United States Energy Information Administration, "CO<sub>2</sub> Emissions from Fuel Combustion," 2016. Accessed on: 2019 Aug 10. Available at: <https://www.iea.org/publications/freepublications/publication/CO2EmissionsfromFuelCombustionHighlights2017.pdf>

29. Gass V, Schmidt J, Schmid E. Analysis of alternative policy instruments to promote electric vehicles in Austria. *Renew Energ.* 2014;61:96-101.
30. Nanaki EA, Koroneos CJ. Climate change mitigation and deployment of electric vehicles in urban areas. *Renew Energ.* 2016;99:1153-60.
31. Andwari AM, Pesiridis A, Rajoo S, Martinez-Botas R, Esfahanian V. A review of Battery Electric Vehicle technology and readiness levels. *Renew Sustain Energ Rev.* 2017;78:414-30.
32. United States Energy Information Administration, "Global EV Outlook," 2017. Accessed on: 2019 Aug 10. Available at: <https://www.iea.org/publications/freepublications/publication/GlobalEVOutlook2017.pdf>
33. Enerdata, "Global Energy Statistical Yearbook," 2017. Accessed on: 2019 Aug 10. Available at: <https://www.enerdata.net/publications/reports-presentations/global-energy-trends-2017.html>
34. United States Energy Information Administration, "Coal medium-term market report," 2016. Accessed on: 2019 Aug 10. Available at: <http://www.iea.org/Textbase/npsum/MTCMR2016SUM.pdf>
35. REN21, "Renewables 2017 Global Status Report," 2017. Accessed on: 2019 Aug 10. Available at: [http://www.ren21.net/wp-content/uploads/2017/06/17-8399\\_GSR\\_2017\\_Full\\_Report\\_0621\\_Opt.pdf](http://www.ren21.net/wp-content/uploads/2017/06/17-8399_GSR_2017_Full_Report_0621_Opt.pdf)
36. Pflaum P, Alamir M, Lamoudi MY. Battery sizing for PV power plants under regulations using randomized algorithms. *Renew Energ.* 2017;113:596-607.
37. Lee MH, Chang DS. Allocative efficiency of high-power Li-ion batteries from automotive mode (AM) to storage mode (SM). *Renew Sustain Energ Rev.* 2016;64:60-7.
38. Uddin K, Jackson T, Widanage WD, Chouchelamane G, Jennings PA, Marco J. On the possibility of extending the lifetime of lithium-ion batteries through optimal V2G facilitated by an integrated vehicle and smart-grid system. *Energy.* 2017;133:710-22.
39. Weiller C, Sioshansi R. The role of plug-in electric vehicles with renewable resources in electricity systems. *Revue d'économie industrielle.* 2014;(148):291-316.
40. Hennings W, Mischinger S, Linssen J. Utilization of excess wind power in electric vehicles. *Energy Pol.* 2013;62:139-44.
41. Dias MV, Haddad J, Nogueira LH, da Costa Bortoni E, da Cruz RA, Yamachita RA, Goncalves JL. The impact on electricity demand and emissions due to the introduction of electric cars in the São Paulo Power System. *Energy Pol.* 2014;65:298-304.
42. McLaren J, Miller J, O'Shaughnessy E, Wood E, Shapiro E. CO2 emissions associated with electric vehicle charging: the impact of electricity generation mix, charging infrastructure availability and vehicle type. *The Elec J.* 2016;29(5):72-88.
43. Hafez O, Bhattacharya K. Optimal design of electric vehicle charging stations considering various energy resources. *Renew Energ.* 2017;107:576-89.

44. Zhang Q, Tezuka T, Ishihara KN, Mclellan BC. Integration of PV power into future low-carbon smart electricity systems with EV and HP in Kansai Area, Japan. *Renew Energ.* 2012;44:99-108.
45. Ramachandran S, Stimming U. Well to wheel analysis of low carbon alternatives for road traffic. *Energ Environ Sci.* 2015;8(11):3313-24.
46. Degirmenci K, Breitner MH. Consumer purchase intentions for electric vehicles: is green more important than price and range?. *Transport Res Transport Environ.* 2017;51:250-60.
47. Axsen J, Kurani KS. Connecting plug-in vehicles with green electricity through consumer demand. *Environ Res Lett.* 2013;8(1):014045.
48. Wood E. 'Optimized microgrid' at Algonquin College achieves positive ROI. Microgrid Knowledge, 2016 July 29. Accessed on: 2019 Aug 10. Available at: <https://microgridknowledge.com/optimized-microgrid-2/>.
49. Gómez-González M, Ruiz-Rodríguez FJ, Jurado F. Metaheuristic and probabilistic techniques for optimal allocation and size of biomass distributed generation in unbalanced radial systems. *IET Renew Power Gen.* 2015;9(6):653-9.
50. Soltani Z, Ghaljehei M, Gharehpetian GB, Aalami HA. Integration of smart grid technologies in stochastic multi-objective unit commitment: An economic emission analysis. *Int J Electr Power Energy Syst.* 2018;100:565-90.
51. Gan LK, Shek JK, Mueller MA. Hybrid wind–photovoltaic–diesel–battery system sizing tool development using empirical approach, life-cycle cost and performance analysis: A case study in Scotland. *Energ Convers Manag.* 2015;106:479-94.
52. Wenyan L, editor. Risk assessment of power systems: Models, methods, and applications. 2nd ed. Hoboken, NJ: John Wiley & Sons, Inc.; 2014.
53. United States National Renewable Energy Laboratory, Geospatial Data Science Data and Tools, Maps, 2018. Accessed on: 2019 Aug 10. Available at: <https://www.nrel.gov/gis/data-tools.html>.
54. Federal Highway Administration. National Household Travel Survey, U.S. Department of Transportation, Washington, DC, 2017. Accessed on: 2019 Aug 10. Available at: <https://nhts.ornl.gov>
55. Safdarian F, Lamonte L, Kargarian A, Farasat M. Distributed Optimization-Based Hourly Coordination for V2G and G2V. Paper presented at: 2019 IEEE Texas Power and Energy Conference (TPEC); 2019 Feb 7; TX, USA (pp. 1-6). New York: IEEE, 2019.
56. United States Energy Information Administration, "Annual Energy Outlook," 2018. Accessed on: 2019 Aug 10. Available at: <https://www.eia.gov/outlooks/aeo/pdf/AEO2018.pdf>
57. United States Energy Information Administration, "Construction cost data for electric generators." Accessed on: 2019 Aug 10. Available at: <https://www.eia.gov/electricity/generatorcosts/>

58. Mundada AS, Prehoda EW, Pearce JM. US market for solar photovoltaic plug-and-play systems. *Renew Energ.* 2017;103:255-64.
59. Electric Power Research Institute, “Budget for solar PV plant operations & maintenance: practices and pricing,” SAND2016-0649R. Accessed on: 2019 Aug 10. Available at: <http://prod.sandia.gov/techlib/access-control.cgi/2016/160649r.pdf>
60. Hdidouan D, Staffell I. The impact of climate change on the levelised cost of wind energy. *Renew Energ.* 2017;101:575-92.
61. United States Energy Information Administration, “Levelized Cost and Levelized Avoided Cost of New Generation Resources in the Annual Energy Outlook,” 2017. Accessed on: 2019 Aug 10. Available at: [https://www.eia.gov/outlooks/aeo/pdf/electricity\\_generation.pdf](https://www.eia.gov/outlooks/aeo/pdf/electricity_generation.pdf)
62. Geuss M. Electric vehicle price is rising, but cost-per-mile is falling. *Ars Technica*, 2017 Sept 16. Accessed on 2019 Aug 10. Available at <https://arstechnica.com/cars/2017/09/the-average-price-of-electric-cars-rose-in-2016-but-its-not-a-backwards-trend/>.
63. Lambert F. Electric vehicle battery cost dropped 80% in 6 years down to \$227/kWh — Tesla claims to be below \$190/kWh. *Electrek*, 2017 Jan 30. Accessed on: 2019 Aug 10. Available at: <https://electrek.co/2017/01/30/electric-vehicle-battery-cost-dropped-80-6-years-227kwh-tesla-190kwh/>.
64. United States Energy Information Administration, “Overview of the DOE VTO Advanced Battery R&D Program,” 2017. Accessed on: 2019 Aug 10. Available at: [https://energy.gov/sites/prod/files/2016/06/f32/es000\\_howell\\_2016\\_o\\_web.pdf](https://energy.gov/sites/prod/files/2016/06/f32/es000_howell_2016_o_web.pdf)
65. Hagman J, Ritzén S, Stier JJ, Susilo Y. Total cost of ownership and its potential implications for battery electric vehicle diffusion. *Res Bus Manag.* 2016;18:11-7.
66. New York Independent System Operator, “Power Trends: New York’s Evolving Electric Grid,” 2017. Accessed on: 2019 Aug 10. Available at: <https://www.nyiso.com/documents/20142/2223020/2017-Power-Trends.pdf>
67. Olah C. Understanding LSTM networks. *Colah’s Blog*, 2015 Aug 27. Accessed on: 2019 Aug 10. Available at: <https://colah.github.io/posts/2015-08-Understanding-LSTMs/>.
68. Hooshyar H, Mahmood F, Vanfretti L, Baudette M. Specification, implementation, and hardware-in-the-loop real-time simulation of an active distribution grid. *Sustain Energ, Grids and Net.* 2015;3:36-51.
69. Azimian B, Fijani RF, Ghotbi E, Wang X. Stackelberg game approach on modeling of supply demand behavior considering BEV uncertainty. Paper presented at: 2018 IEEE International Conference on Probabilistic Methods Applied to Power Systems (PMAPS); 2018 Jun 24; ID, USA. (pp. 1-6). New York: IEEE, 2018.

70. Ahmadian S, Ebrahimi S, Ghotbi E. Wind farm layout optimization problem using joint probability distribution of CVaR analysis. Paper presented at: 2019 IEEE 9th Annual Computing and Communication Workshop and Conference (CCWC); 2019 Jan 7; NV, USA. (pp. 0007-0012). New York: IEEE, 2019.
71. New York Independent System Operator, Reliability Analysis Data Manual, 2019. Accessed on: 2019 Aug 10. Available at: <https://www.nyiso.com/documents/20142/2924447/rel-anl-data-mnl.pdf>